

The Mathematical Modelling of Waste Fats Treatment into Biogas

Samuel Emebu, MSc, Ph.D.

Doctoral Thesis Summary



Tomas Bata University in Zlín

Faculty of Applied Informatics

Matematické modelování zpracování odpadních tuků na bioplyn

The Mathematical Modelling of Waste Fats Treatment into Biogas

Doctoral thesis summary

Author: **Samuel Emebu, MSc, Ph.D.**

Degree programme: P3902-Engineering Informatics

Degree course: 3902V037E-Automatic Control and Informatics

Supervisor: Assoc. Prof. Ing. Marek Kubalčík, Ph.D.

Consulting Supervisor: Prof. Ing. Dagmar Janáčková, CSc.

External examiners: Prof. Ing. Kolomazník, DrSc.

Assoc. Prof. Ing. Ondřej Vopička, Ph.D.

Assoc. Prof. Ing. Pavel Hrnčíř, Ph.D.

Zlín, November 2023

© Samuel Emebu

Published by **Tomas Bata University in Zlín** in the Edition **Doctoral Thesis Summary**.

The publication was issued in the year 2023.

***Klíčová slova:** Anaerobní digesce, model jednostupňové degradace, hydrolyza lipidů, evoluce bioplynu, dynamika růstu bublin, odpařování vody, dynamika pH.*

***Keywords:** Anaerobic digestion, single-step-degradation model, lipid hydrolysis, biogas evolution, bubble growth dynamics, water evaporation, pH dynamics*

Full text of the doctoral thesis is available in the Library of TBU in Zlín.

ISBN 978-80-7678-219-8

Abstract

The need to supplement or replace fossil energy consumption to enhance energy supply has prompted renewable energy development. Especially from biomass degradation, since it is advantageous for its ability to tackle the challenges of energy security and waste management simultaneously. Specifically, the anaerobic digestion (AD) of biomass (lipid) into biogas has been considered. The work highlighted the current state-of-the-art AD models (single-equation model and multi-step dynamic model) with a specific interest in single-step-degradation model (SSDM) a multi-step dynamic model. The SSDM was modelled in such a way that it could be easily applied to control the pressure, pH, and temperature of the AD. Therefore, in addition to modelling the biochemical stage, other processes such as hydrolysis of lipid, mass transfer, heat transfer, and pH of the process were modelled, together with the necessary microbial activity, physicochemical, and thermodynamic parameters modelled as a function of temperature, as well as pressure. Additionally, the biogas bubble growth and motion dynamics, which enable the estimation of biogas bubble diameter, rising velocity, pressure inside and on the bubble at the gas-liquid interface, were also estimated. Most processes considered in the SSDM were modelled theoretical based on data from literature. However, the hydrolysis process involving the degradation of lipid into LCFA, and glycerol was experimentally modelled as a function of temperature (25 to 50 °C), and the model showed excellent proximity with experimental data, as well as its optimal temperature found to be 45 °C. Having modelled all processes to be considered in the SSDM, the model was simulated in MATLAB for different scenarios, to effectively evaluate its robustness. These scenarios involved evaluating the performance of the SSDM to analyse the effect of pressure (i.e., over-, atmospheric-, and under-pressure) temperature (i.e., 35, 45, and 60 °C), pH on the biogas production, as well as a simplified comparison with the experimental production of biogas at atmospheric pressure. Based on these analyses and comparisons it was found that the developed SSDM was quite adequate to predict the AD of lipid into biogas. Although beyond the scope of this work, it was proposed that further comprehensive comparison or optimisation of the model to real-time experimental data of substrate, microbes, dissolved and evolved biogas species concentrations, as well as water vapour together with biogas water content maybe be necessary to fully validate the model.

Abstrakt

Potřeba doplnit nebo nahradit spotřebu fosilní energie za účelem zvýšení dodávek energie podnítila rozvoj výroby obnovitelné energie, a to zejména s využitím degradace biomasy. Tento způsob výroby energie je výhodný z hlediska výzev energetické bezpečnosti a nakládání s odpady. Práce se zabývá modelováním anaerobní digesce (AD) biomasy (lipidů) na bioplyn s využitím současných nejmodernější AD modelů (jednorovnicový model a vícekrokový dynamický model). Zvláštní důraz je kladen na jednostupňový degradační model (SSDM), vícestupňový dynamický model. SSDM byl modelován takovým způsobem, že jej bylo možné snadno použít pro simulaci řízení tlaku, pH a teploty AD. Proto byly kromě modelování biochemické fáze modelovány další procesy, jako je hydrolyza lipidů, přenos hmoty, přenos tepla a pH procesu, spolu s nezbytnou mikrobiální aktivitou, fyzikálně-chemickými a termodynamickými parametry modelovanými jako funkce teploty a tlaku. Dále byl odhadnut růst a dynamika pohybu bublin bioplynu, která umožňuje odhadnout průměr bublin bioplynu, rychlost stoupaní, tlak uvnitř a na bublině na rozhraní plyn-kapalina. Většina procesů uvažovaných v SSDM byla modelována teoreticky na základě dat z literatury. Proces hydrolyzy zahrnující degradaci lipidů na LCFA a glycerol byl modelován experimentálně v závislosti na teplotě (25 až 50 °C) a model vykazoval velmi dobrou shodu s experimentálními daty. Optimální teplota procesu byla experimentálně stanovena jako 45 °C. Po namodelování všech dílčích procesů, které jsou uvažovány v SSDM, byl celkový model simulován v MATLABu pro různé scénáře, aby bylo možno efektivně vyhodnotit jeho robustnost. Tyto scénáře zahrnovaly vyhodnocení efektivity produkce bioplynu s využitím SSDM v závislosti na tlaku (tj. přetlaku, atmosférického a podtlaku), teplotě (tj. 35, 45 a 60 °C). Bylo rovněž provedeno zjednodušené srovnání s experimentální výrobou bioplynu za atmosférického tlaku. Na základě těchto analýz a srovnání bylo zjištěno, že vyvinutý SSDM je zcela adekvátní pro predikci AD lipidů do bioplynu. I když je to nad rámec této práce, model byl navržen tak, aby bylo možno provést další komplexní srovnání nebo optimalizaci modelu na experimentální data substrátu, mikrobů, rozpuštěných a vyvinutých druhů bioplynu, jakož i vodní páry spolu s obsahem vody v bioplynu v reálném čase, což je nutné ke komplexnímu ověření modelu.

Acknowledgement

My appreciation goes to God for inspiration, perseverance, as well as strength throughout this programme. I also appreciate my supervisors' doc. Ing. Marek Kubalčík, Ph.D., and Prof. Ing. Dagmar Janáčková, CSc., for giving me the opportunity to undertake this thesis, their valuable advice and professional guidance. I also appreciate the immense contribution of doc. Ing. Jiří Pecha, Ph.D., for his theoretical and experimental advice as well as Ing. Lubomír Šánek, Ph.D. and Ing. Jakub Husár for their experimental and miscellaneous contributions. Furthermore, I appreciate the Internal Grant Competition of the Tomas Bata University (UTB) (i.e., CebiaTech/2021/002, CebiaTech/2022/002, and CebiaTech/2023/004), the UTB, and the Faculty of Applied Informatics (FAI) scholarship boards for financial support. Appreciation also goes to the entire Faculty of Applied Informatics for their various administrative as well technical support.

Finally, I appreciate my wife (Mrs. Oluchi Emebu), my mother (Mrs. Martina Emebu), and other family members as well as friends for their prayers, emotional support, and patience during this programme.

Table of contents

1. Introduction.....	1
1.1. Current state of the issues-Research overview.....	2
1.2. Aims and objectives.....	4
2. Summary of anaerobic digestion.....	5
2.1. Stages in anaerobic digestion.....	5
2.1.1. Hydrolysis of feedstock.....	5
2.1.2. Acidogenesis of hydrolysis products.....	5
2.1.3. Acetogenesis of products from acidogenesis.....	6
2.1.4. Methanogenesis of products from acetogenesis.....	6
3. Model review on anaerobic digestion.....	7
3.1. Single-step-degradation model.....	7
3.2. Two-step-degradation model.....	7
3.3. Multi-step-degradation model.....	8
3.4. Theoretical estimation of substrate, microbes, and biogas yield.....	8
4. Theoretical framework – Model development.....	9
4.1. Experimental analysis of lipid hydrolysis.....	14
5. Experimental framework – Materials and methods.....	15
5.1. Collection and storage of sludge sample.....	15
5.2. Dispersion of lipid sample in sludge.....	15
5.3. Setup of the anaerobic hydrolysis system.....	15
5.4. Analysis of hydrolysed lipid.....	16
5.5. Modelling lipid hydrolysis kinetics.....	16
5.6. Evaluation of models.....	17
5.7. Simulation of model.....	17
6. Results.....	19
6.1. Hydrolysis kinetics.....	19
6.2. Anaerobic digestion simulation.....	20
6.2.1. Effect of pressure.....	20

6.2.2. Effect of pH inhibition.....	26
6.2.3. Effect of temperature	28
7. Conclusion	33
7.1. Contribution to science and practice.....	34
Bibliography	35
Appendix	37
List of figures.....	41
List of tables	43
List of Abbreviations	43
List of symbols	44
List of subscripts.....	48
List of publications	48
Curriculum vitae	50

1.Introduction

Energy is the currency of all motive physical, chemical, and physiochemical activities within biological, as well as non-biological systems. In the process industry, energy is particularly useful in transforming raw materials to finish products, hence the need to source and store it. Energy can be generated from diverse sources, which can be classified into renewable (e.g., biomass, solar, etc.) and fossil-based energy sources (Petroleum, coal, etc.). Although as of the year 2021, fossil fuel (about 82%) remains the most utilised source of energy worldwide, they are considered unclean energy sources due to their high carbon footprint on global warming [1,2]. However, sequel to the aftermath of the 2022 global energy crisis, which also spilled over to 2023 [3]. There have been accelerated efforts to simultaneously reduce fossil energy consumption, and develop renewable energy resources, as a supplementary energy source to ensure a nation's energy security. Considering that nations are also faced with the challenges of waste generation, treatment, and disposal. It is therefore necessary to consider energy generation from waste [4,5], as a viable means to tackle energy security as well as waste generation. Fundamentally, energy security and waste management are critical global security, economic, and environmental reoccurring issues that require persistent solutions. Energy security is a combination of all deliberate actions taken by necessary stakeholders, to ensure that the energy sources of a nation are diversified and constantly available to meet energy demand in both normal and critical conditions. Apart from tackling the challenges of energy security and waste management, renewable energy from waste also offers the synergy of mitigating climate change and reducing the emission of air pollutants that would have resulted from using fossil energy sources [1,6].

Considering the earlier highlighted challenges of energy security and waste management, it makes sense to seriously consider this route for renewable energy generation. This assertion is evident in the reported claim that the energy contribution of biomass to the world's renewable energy utilisation constitutes approximately 55%, and over 6% of the global energy supply[7]. Conversion of biomass to refined forms, "biofuel" is required for uses in different processes, and this can be achieved using different methods, categorised as, thermal, chemical, and biochemical methods [8]. Biochemical conversion method would however be considered. This is because, compared with other methods, the biochemical method is advantageous for reasons such as mild temperature and normal pressure conditions, low equipment cost, low energy, little dependence on chemicals, high specificity of biomass conversion to biofuel, and usability of unutilised biomass (digestate) as organic fertilizer [9].

1.1. Current state of the issues-Research overview

Considering the earlier highlighted advantages of biochemical conversion of biomass to biofuel, in this work the anaerobic digestion of biomass to biogas would be considered. Anaerobic digestion is specifically considered because it can utilise the most variety of organic matter (such as waste material unsuitable to produce other biofuels, typically waste with a high percentage of organic biodegradable matter and high moisture content) [10], hence also suitable for efficient waste management. Its energy yield per square meter of feedstock is higher and more efficient for energy production than other biofuels (i.e., liquid biofuels such as bioethanol, and biodiesel). Although, while the convenience and energy density of liquid biofuels is admirable for some purposes, if energy recovery from biomass is to be maximised, then biogas production is the best choice. Also, for situations where bioethanol and biodiesel production are required, biogas can be produced from their waste products and as such improves the energy yield of the production process [11]. Furthermore, considering the earlier highlighted fact that lipid has more energy density than other feedstock, in addition to the fact that lipid-rich waste especially when mixed with a high percentage of organic biodegradable matter as well as high moisture content [10], and unsuitable for biodiesel production due to high content Free fatty acid is generated daily in large amounts from food processing companies (edible oil processing plant, dairy plant, slaughterhouses, etc.), cooking waste from hospitality industry (hotels, restaurants, etc.), together with domestic residences [12].

Anaerobic digestion on a holistic view is a simple process, however, on an intricate level, it involves four complex biochemical reaction stages: hydrolysis; acidogenesis, acetogenesis; and methanogenesis, to produce biogas. The biogas produced is usually composed of approximately 50 – 75% methane (CH_4), carbon dioxide (CO_2), and impurities such as 0–5% nitrogen, 0–5000 ppm hydrogen sulphide (H_2S), trace amount of hydrogen, carbon monoxide, and moisture [13]. The amount and composition of biogas produced depends on the efficiency of the biochemical and mass transfer processes in AD. These processes are affected by factors such as temperature, partial pressure of biogas species, and pH. And these highlighted factors determine efficiency based on how they influence the degree of stability (i.e., optimal condition) of AD. Therefore, mathematical models that relate these factors to feedstock and intermediates digestion, and production of biogas, are usually required to physically describe these influences, monitor the process (e.g., deduce the rate-limiting step), as well as optimise, and control the stability of AD [14]. Note that to ensure a comprehensive description of the AD, these mathematical models should be able to physically interpret the main processes in the AD, i.e., the earlier highlighted biochemical reaction stages, in addition to other processes such

as mass and heat transfers, and physicochemical processes (e.g., pH dynamics). Also crucial are auxiliary models to estimate vital parameters (microbial activity parameters, microbe, biogas yields, etc.) needed in the computation of models for the earlier highlighted main processes. Model development for such a comprehensive description of AD would enhance the robustness of the physical interpretation of the AD process and enable the evaluation of certain phenomena, such as the rate-limiting step of the process. Typically, in analysing the rate-limiting step (i.e., the slowest process) in AD, literature reports have debated that the hydrolysis-, methanogenesis-stage, or mass transfer of biogas could be the rate-limiting step [15,16], therefore adequately modelling these steps is important.

There are numerous mathematical models for AD reported in literature, and they include the popular Anaerobic Digestion Model No. 1 (ADM1) [17], Gaussian, Gompertz, multi-regression, acidogenesis-methanogenesis-two-steps (AM2) models, etc. [18–21]. These models are uniquely different in their overall approach (mechanistic or statistical), initial assumptions, process phenomena, and the biochemical stages considered in their development. In general, AD models can be categorized into single-equation and multi-step dynamic models. The single-equation model could be developed as dynamic- or cumulative single-equation model, which could either be considered as a simple-linear, -nonlinear, or multi-regression single-equation model. While the multi-step dynamic model could be modelled as, single-step-degradation model (SSDM), two-step-degradation model (TSDM), and multi-step-degradation model (MSDM) [22]. These classes of models have the specialty, advantages, and disadvantages as described in literature [22]. In general, most single-equation models are simple, require few numbers, and inexpensive experiments to develop. In contrast, multi-step dynamic models are complex, but more accurate, with their complexity as well as accuracy in the order of MSDM > TSDM > SSDM, and require a substantial number of experiment data, as well as procedures, which maybe expensive. In summary, when simplicity, time-, cost-constraint, and not accuracy are priorities, the single-equation model would be preferred over the multi-step dynamic model [22]. Although, it is worth noting that while the single-equation model is less accurate than its counterpart, resulting data (e.g., biogas production potential, maximum biogas production rate) from its models are useful and suitable for preliminary investigation. Furthermore, while multi-step dynamic models are complex, time-consuming, and expensive to develop, they can be consolidated with numerous dynamic models of other main processes (i.e., mass and heat transfers, etc.) and auxiliary models (i.e., models for microbial activity parameters, microbe-, and biogas-yields, etc.). As such resulting in a clearer physical interpretation of the AD process. Therefore, in this work, the multi-step dynamic model would be applied, specifically, the SSDM will be applied because it is simpler and quicker to evaluate unknown parameters, due to its fewer dynamic equations

than the other models. The SSDM would be developed with consideration to easily apply it to control the pressure, pH, and temperature of the AD process.

1.2.Aims and objectives

Therefore, this work aims to theoretically model a single-step-degradation model (SSDM) to describe the anaerobic digestion of lipid-rich waste into biogas. In addition to experimentally investigate as well as model the kinetic of lipid hydrolysis into LCFA, and glycerol with incorporation of the effect of temperature. Further with the application of the lipid hydrolysis kinetic into the SSDM. Therefore, the scope of the work entails the following objectives:

1. Source for, prepare, and characterise suitable industrial anaerobic sludge.
2. Propose a suitable experimental setup for anaerobic digestion experiments.
3. Homogenise stabilise lipid in the aqueous sludge sample.
4. Develop methodologies to determine qualitative and quantitatively describe lipid degradation in AD.
5. Investigate and develop a model to describe lipid hydrolysis kinetics in AD at different temperatures.
6. Curve-fit model or source for reported models to describe essential physiochemical (e.g., density), thermodynamic (e.g., specific heat capacity), and biochemical (e.g., microbe specific growth rate) parameters as a function of temperature, and/or pressure.
7. Develop a unique SSDM to describe lipid anaerobic digestion into biogas.
8. Validate the developed models for lipid hydrolysis kinetics as well as the SSDM via comparison with experimental results using adequate statistical tools when applicable.

2.Summary of anaerobic digestion

Anaerobic digestion (AD) is a simple process, yet involves complex biochemical reactions made possible by a group of microbes that works both independently and collectively to metabolise feedstocks to a mixture of gases (mostly CH₄ & CO₂) in the absence of oxygen.

2.1.Stages in anaerobic digestion

AD processes can be divided into two categories: Extracellular steps (pretreatment and hydrolysis processes) and Intracellular steps (acidogenesis, acetogenesis, and methanogenesis), as illustrated in Figure (2.1). Where LCFA – long chain fatty acids, and VFA – volatile fatty acids. And for consistency and clarity, the reaction schemes in each stage shall be illustrated with lipid feedstock.

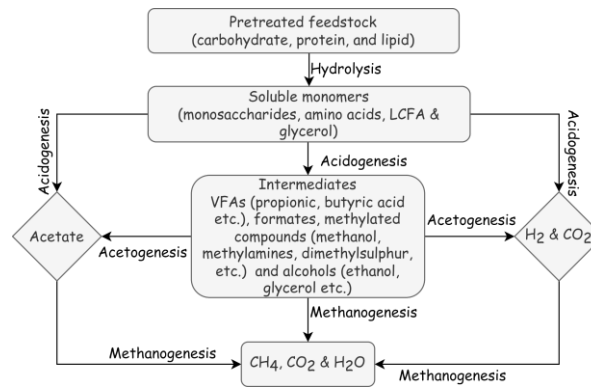
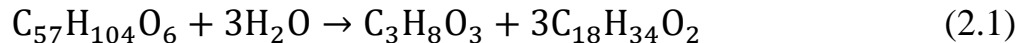


Figure 2.1. Illustrative scheme of anaerobic digestion stages [22]

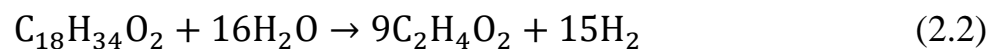
2.1.1.Hydrolysis of feedstock

Equation (2.1) is a typical illustration of the hydrolysis of lipids (F) into glycerol (S₁) and fatty acids (S₂).



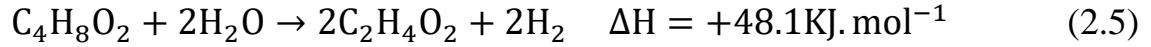
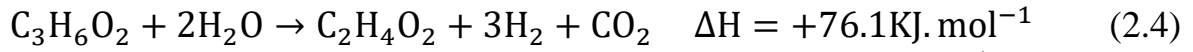
2.1.2.Acidogenesis of hydrolysis products

Equations (2.2) and (2.3), respectively illustrate the acidogenesis of fatty LCFA (oleic fatty acid) and glycerol without microbes' activities.



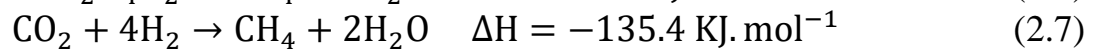
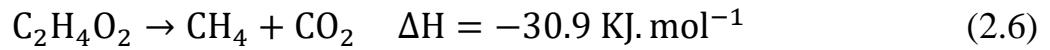
2.1.3. Acetogenesis of products from acidogenesis

Equations (2.4) and (2.5), illustrate the acetogenesis of propionic, and butyric acid into acetic acid, carbon dioxide, as well as hydrogen, without microbes' activities.



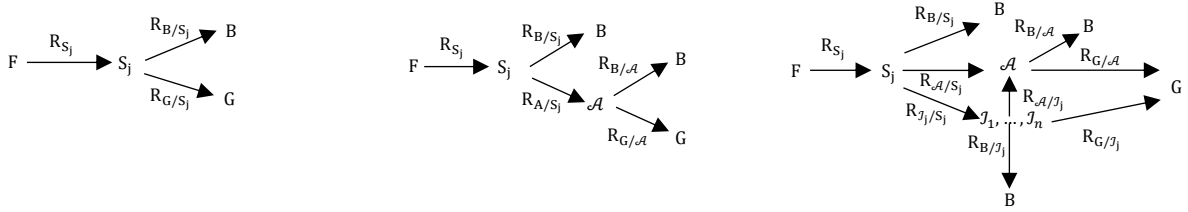
2.1.4. Methanogenesis of products from acetogenesis

Equations (2.6) and (2.7), illustrate methanogenesis from Acetoclastic and Hydrogenotrophic methanogens respectively, without microbes' activities.



3. Model review on anaerobic digestion

Popular models for AD highlighted in literature can be grouped into single-equation model and multi-step dynamic model as proposed by Emebu et al. [22]. The multi-step dynamic models shall be of focus as illustrated in Figure (3.1), and Equations (3.1) – (3.20). The generalised Continuous Stirred Tank Reactor (CSTR) type bioreactor is used for illustration. Where $j = 1, 2, \dots, n$ indicates the number of species being considered, i.e. various substrates, S_j (e.g. LCFA and glycerol from lipid feedstock, with input composition, $S_{i,j}$), intermediates, J_j (VFAs, alcohol, etc., with input composition, $J_{i,j}$), biogas constituents, G_j (e.g. CH_4 , CO_2 , H_2 , etc.,) in the process, and \mathcal{D} is the bioreactor dilution rate, a ratio of input flowrate and bioreactor volume.



a. Single-Step Degradation b. Two-Step-Degradation c. Multi-Step Degradation

Figure 3.1. Illustration of degradation level considered in the multi-step dynamic models

3.1. Single-step-degradation model

The SSDM is a simplified model of biogas yield from the substrate, S_j , as illustrated by Equation (3.1), a generic expression, and the SSDM has been reported in literature [23].

$$dS_j/dt = \mathcal{D}(S_{i-j} - S_j) + R_{S_j} - R_{B/S_j} - \sum_{j=1}^n R_{G_j/S_j} \quad (3.1)$$

3.2. Two-step-degradation model

The TSDM also referred to as the AM2 model (Acidogenesis methanogenesis, two-step model) is popularly reported in literature [20,21], and it models the yield of biogas from acetic acid, \mathcal{A} , formed from substrates, S_j , Equation (3.2) – (3.3).

$$dS_j/dt = \mathcal{D}(S_{i-j} - S_j) + R_{S_j} - R_{B/S_j} - R_{\mathcal{A}/S_j} \quad (3.2)$$

$$d\mathcal{A}/dt = \mathcal{D}(\mathcal{A}_i - \mathcal{A}) + R_{\mathcal{A}/S_j} - R_{B/A} - \sum_{j=1}^n R_{G_j/\mathcal{A}} \quad (3.3)$$

3.3. Multi-step-degradation model

The MSDM is popularly reported in literature [17], and the ADM1 is an example of this model. It also models the yield of biogas from acetic acid, \mathcal{A} , formed from intermediates, \mathcal{J}_j (VFAs, alcohols, etc) generated from substrates, S_j degradation, Equation (3.4) – (3.6).

$$dS_j/dt = \mathcal{D}(S_{i-j} - S_j) + R_{S_j} - R_{B/S_j} - R_{\mathcal{A}/S_j} - \sum_{j=1}^n R_{\mathcal{J}_j/S_j} \quad (3.4)$$

$$d\mathcal{J}_j/dt = \mathcal{D}(\mathcal{J}_{i-j} - \mathcal{J}_j) + R_{\mathcal{J}_j/S_j} - R_{B/\mathcal{J}_j} - R_{\mathcal{A}/\mathcal{J}_j} - \sum_{j=1}^n R_{G_j/\mathcal{J}_j} \quad (3.5)$$

$$d\mathcal{A}/dt = \mathcal{D}(\mathcal{A}_i - \mathcal{A}) + R_{\mathcal{A}/S_j} + R_{\mathcal{A}/\mathcal{J}_j} - R_{B/\mathcal{A}} - \sum_{j=1}^n R_{G_j/\mathcal{A}} \quad (3.6)$$

3.4. Theoretical estimation of substrate, microbes, and biogas yield

The generic expressional statement for the transformation of organic matter in AD is given by Equation (3.7). Typical estimated essential theoretical yield of substrate, microbes, and biogas from lipid are given in Table (3.1).

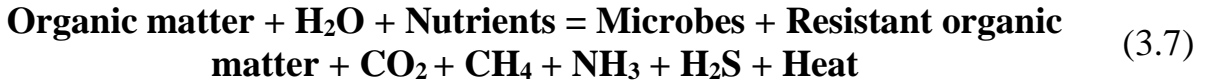


Table 3.1. Theoretical yield estimate of the substrate from feedstock, biogas and microbes from the substrate, ammonia from microbes for lipid (triglyceride with oleic acid)

Yield (Kg.kg ⁻¹)	S _j =LCFA, C ₁₈ H ₃₄ O ₂	S _j =Glycerol, C ₃ H ₈ O ₃
Feed, Y _{S_j/F}	0.9570	0.1041
Microbes, Y _{B_j/S_j}	1.5680	0.8010
NH ₃ from microbes, Y _{G_DNH₃*/B_j}	0.1384	0.1383
CH ₄ , Y _{G_DCH₄/S_j}	0.7234	0.3043
CO ₂ , Y _{G_DCO₂/S_j}	0.8191	0.5978
H ₂ , Y _{G_DH₂/S_j}	0.1064	0.0071

4. Theoretical framework – Model development

Considering the SSDM is simpler and quicker to evaluate its parameters, in addition to an easy application for control of pressure, pH, as well as the temperature of the AD. An SSDM is developed based on the description of the highlighted CSTR bioreactor, Figure (4.1).

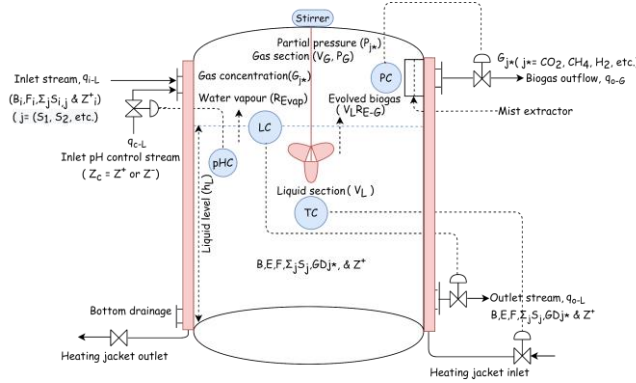


Figure 4.1. Description of anaerobic digestion in a continuous stirred tank reactor (CSTR) type bioreactor with material and heat transfer.

The Equation (4.1) – (4.38) are the dynamics, and necessary auxiliary equations (i.e., analytical, as well as curve fitted models) solved to simulate the AD.

Bioreactor volume, V_R (m^3)

$$V_R = V_L(t) + V_G(t) = \pi r_{Ri}^2 h_L(t) = \pi r_{Ri}^2 h_L(t) + V_G(t) \quad (4.1)$$

Dynamics of liquid volume, dV_L/dt ($m^3 \cdot s^{-1}$)

$$\frac{dV_L}{dt} = q_{i-L} + q_{c-L} - q_{o-L} - (V_L R_{E-G} + R_{Evap} + q_{o-GG} W_{H_2O}) / \rho_L \quad (4.2)$$

Dynamics of liquid level, dh_L/dt ($m \cdot s^{-1}$)

$$\frac{dh_L}{dt} = \frac{q_{i-L} + q_{c-L} - q_{o-L} - (V_L R_{E-G} + R_{Evap} + q_{o-GG} W_{H_2O}) / \rho_L}{\pi r_{Ri}^2} \quad (4.3)$$

Dynamic of gas-vapour headspace volume, dV_G/dt ($m^3 \cdot s^{-1}$)

$$\frac{dV_G}{dt} = q_{o-L} - q_{i-L} + q_{c-L} + (V_L R_{E-G} + R_{Evap} + q_{o-GG} W_{H_2O}) / \rho_L \quad (4.4)$$

Dynamics of lipid degradation, dF/dt ($kg \cdot m^{-3} \cdot s^{-1}$)

$$\frac{dF}{dt} = \frac{q_{i-L}}{V_L} (F_i - F) - \frac{q_{c-L}}{V_L} F + \frac{F}{\rho_L} \left(R_{E-G} + \frac{R_{Evap}}{V_L} + q_{o-GG} W_{H_2O} \right) - K_{lipid} F \quad (4.5)$$

Dynamics of microbe's growth, dB/dt ($kg \cdot m^{-3} \cdot s^{-1}$)

$$\frac{dB}{dt} = \frac{q_{i-L}}{V_L} (B_i - B) - \frac{q_{c-L}}{V_L} B_j + \frac{B}{\rho_L} \left(R_{E-G} + \frac{R_{Evap}}{V_L} + q_{o-GG} W_{H_2O} \right) + (\mu - K_d) B \quad (4.6a)$$

$$\mu_j = \mu_{\max-j} \frac{S_j}{K_{S_j} + S_j} \quad (4.6b)$$

$$\mu_{\max-j} = \{\mathcal{B}_{1-j}(T - T_{\min-j})\}^2 \{1 - \exp[\mathcal{B}_{2-j}(T - T_{\max-j})]\}^2 \quad (4.6c)$$

$j = 1$ for LCFA, and 2 for glycerol; $\mu = \mu_1 + \mu_2$ and $K_d = K_{d-1} + K_{d-2}$

Dynamics of substrate utilisation, dS_j/dt ($\text{kg.m}^{-3}.\text{s}^{-1}$)

$$\begin{aligned} \frac{dS_j}{dt} = & \frac{q_{i-L}}{V_L} (S_{i-j} - S_j) - \frac{q_{c-L}}{V_L} S_j + \frac{S_j}{\rho_L} \left(R_{E-G} + \frac{R_{Evap}}{V_L} + q_{o-GG} W_{H_2O} \right) \\ & + Y_{S_j/F} K_{lipid} F - \frac{\mu_j B}{Y_{B_j/S_j}} \end{aligned} \quad (4.7)$$

Dynamics of biogas in liquid phase, dG_{Dj^*}/dt ($\text{kg.m}^{-3}.\text{s}^{-1}$)

$$\begin{aligned} \frac{dG_{Dj^*}}{dt} = & -\frac{q_{i-L}}{V_L} G_{Dj^*} - \frac{q_{c-L}}{V_L} G_{Dj^*} + \frac{G_{Dj^*}}{\rho_L} \left(R_{E-G} + \frac{R_{Evap}}{V_L} + q_{o-GG} W_{H_2O} \right) + R_{G_{Dj^*}} \\ & - R_{E-j^*} \end{aligned} \quad (4.8a)$$

$$R_{G_{Dj^*}} = (Y_{G_{Dj^*/S_1}} \dot{i}_{pH-j^*}) \left(\frac{\mu_1 B}{Y_{B/S_1}} \Phi_v \right) + (Y_{G_{Dj^*/S_2}} \dot{i}_{pH-j^*}) \left(\frac{\mu_2 B}{Y_{B/S_2}} \Phi_v \right) \quad (4.8b)$$

$$\dot{i}_{pH-j^*} = \frac{1 + 2(10^{0.5(pH_{II} - pH_{ul})})}{1 + 10^{(pH - pH_{ul})} + 10^{(pH_{II} - pH)}} \quad (4.8b)$$

$j^* = \text{CH}_4, \text{CO}_2 \text{ \& } \text{H}_2$; $\Phi_v = \Phi_G$ for $\text{CH}_4 \text{ \& } \text{CO}_2$ and $\Phi_v = \Phi_B$ for H_2

Dynamics of biogas in the headspace, dG_{j^*}/dt ($\text{kg.m}^{-3}.\text{s}^{-1}$)

$$\begin{aligned} \frac{dG_{j^*}}{dt} = & \frac{G_{j^*}}{V_G} (q_{i-L} + q_{c-L} - q_{o-L} - q_{o-G}) \\ & - \frac{G_{j^*}}{\rho_L V_G} (V_L R_{E-G} + R_{Evap} + q_{o-GG} W_{H_2O}) + \frac{V_L}{V_G} R_{E-j^*} \end{aligned} \quad (4.9)$$

Dynamics of biogas partial pressure in headspace, dP_{j^*}/dt ($\text{pa}.\text{s}^{-1}$)

$$\begin{aligned} \frac{dP_{j^*}}{dt} = & \frac{RT}{V_G M_{j^*}} (V_L R_{E-j^*} - q_{o-G} G_{j^*}) \\ & - \frac{P_{j^*}}{V_G} [q_{o-L} - q_{i-L} - q_{c-L} + (V_L R_{E-G} + R_{Evap} + q_{o-GG} W_{H_2O}) / \rho_L] \end{aligned} \quad (4.10)$$

Partial pressure of water vapour, P_{sw} (pa)

$$P_{sw} = \exp \left(73.96 - \frac{7258.2}{T(^{\circ}\text{C}) + 273.15} + 2.276 \times 10^{-3} T(^{\circ}\text{C}) - 7.3073 \ln(T(^{\circ}\text{C}) + 273.15) + 4.1653 \times 10^{-6} T(^{\circ}\text{C})^2 \right) \quad (4.11)$$

Dynamics of water in liquid phase, dw/dt ($\text{kg.m}^{-3}.\text{s}^{-1}$)

$$\begin{aligned} \frac{dw}{dt} = & \frac{q_{i-L}}{V_L} (w_i - w) + \frac{q_{c-L}}{V_L} (w_c - w) + \frac{w}{\rho_L} \left(R_{E-G} + \frac{R_{Evap}}{V_L} + q_{o-G} W_{H_2O} \right) \\ & - \frac{R_{Evap}}{V_L} - \frac{q_{o-GG} W_{H_2O}}{V_L} \end{aligned} \quad (4.12)$$

Dynamics of water vapour in the headspace, dw_v/dt ($\text{kg.m}^{-3}.\text{s}^{-1}$)

$$\frac{dw_v}{dt} = \frac{w_v}{V_G} (q_{i-L} + q_{c-L} - q_{o-L} - q_{o-G}) - \frac{w_v}{\rho_L V_G} (V_L R_{E-G} + R_{Evap} + q_{o-GG} W_{H_2O}) + \frac{R_{Evap}}{V_G} \quad (4.13)$$

Rate of evaporation, R_{Evap} (kg.s⁻¹)

$$R_{Evap} = \frac{\frac{M_w P_{sw}}{RT} \left[q_{o-L} - q_{i-L} - q_{c-L} + \frac{V_L}{\rho_L} R_{E-G} + \frac{q_{o-GG} W_{H_2O}}{\rho_L} \right] + q_{o-G} w_v}{\left(1 - \frac{M_w P_{sw}}{\rho_L RT} \right)} \quad (4.14)$$

Biogas water content, (kg H₂O per m³ biogas/gases)

$$W_{H_2O} = 0.76190042 \left(\frac{P_{sw}}{\phi_{H_2O} P} \right) \exp \left(\frac{(P - P_{sw}) v_{H_2O}}{8314(T + 273.15)} \right) \quad (4.15a)$$

$$\phi_{H_2O} = \exp \left[\left(0.069 - \frac{30.905}{T(^{\circ}C) + 273.15} \right) (10^{-6} P) + \left(\frac{0.3179}{T(^{\circ}C) + 273.15} - 0.0007654 \right) (10^{-6} P)^2 \right] \quad (4.15b)$$

$$v_{H_2O} = -0.5168 \times 10^{-2} + 3.036 \times 10^{-4} T(^{\circ}C) + 1.784 \times 10^{-6} T(^{\circ}C)^2 \quad (4.15c)$$

Water content accompanying biogas outflow, \dot{m}_{o-Gw} (kg.s⁻¹)

$$\dot{m}_{o-Gw} = q_{o-GG} W_{H_2O} \quad (4.16)$$

$q_{o-GG} = \delta_G q_{o-G} G$; $\delta_G = RT/M_G P_G$ and $P_G = (P_{CH_4} + P_{CO_2} + P_{H_2} + P_{N_2} \dots)$; $G = \sum_{j^*} J^* G_{j^*}$ i.e., $J^* = CH_4, CO_2, H_2,$ and N_2

Biogas evolution rate, R_{E-j^*} (kg.m⁻³.s⁻¹)

$$R_{E-j^*} = (K_L a)_{j^*} (G_{Dj^*} - K_{Hj^*} P_{j^*}) \quad (4.17)$$

Henry's constant for biogas species, K_{Hj^*} (kg.m⁻³.pa⁻¹)

$$K_{Hj^*} = \left(\frac{M_{j^*}}{101325} \right) \exp \left\{ \frac{-\Delta \psi_{j^*}^{ovl}}{0.0821T} \right\} \quad (4.18)$$

Mass transfer coefficient, $(K_L a)_{j^*}$ (s⁻¹)

$$(K_L a)_{j^*} = (K_L a)_{H_2} (D_{Lj^*} / D_{LH_2})^{0.5} \quad (4.19)$$

Diffusivity of biogas species, D_{Lj^*} (m².s⁻¹)

$$D_{Lj^*} = 6.43012 \times 10^{-8} \frac{q_L^{0.36} \exp(-2539/T)}{\eta_L^{0.61} q_{j^*}^{0.64}} \quad (4.20)$$

$q_L = 0.0187$, q_{j^*} , $j^* = CH_4, CO_2,$ & H_2 0.0377, 0.0373, & 0.0143 m³.kgmole⁻¹

Partial pressure inside biogas bubble species, dp_{j^*}/dt (pa.s⁻¹)

$$\frac{dp_{j^*}}{dt} = \frac{6}{\pi d_{j^*}^3} \left[RT \frac{dn_{j^*}}{dt} - \frac{p_{j^*} \pi d_{j^*}^2}{2} \frac{d(d_{j^*})}{dt} \right] \quad (4.21)$$

Biogas bubble sizes i.e., diameter (m.s⁻¹)

$$\frac{d(d_{j^*})}{dt} = \frac{2}{\pi d_{j^*}^2 P_{T-j^*}} RT \frac{dn_{bj^*}}{dt} \quad (4.22)$$

Pressure on biogas bubble species, p_{T-j^*} (pa.s⁻¹)

$$p_{T-j_*} = P + \rho_L g(h_L - h_{j_*}) + \frac{4\gamma_{Lj_*}}{d_{j_*}} \quad (4.23)$$

Interfacial tension, γ_{LCH_4} (N.m⁻¹) via Table (4.1)

$$\gamma_{LCH_4} = 1.11 \times 10^{-4} (\rho_L - \rho_{CH_4})^{1.024} (T/T_{C-CH_4})^{-1.25} \quad (4.24)$$

$$\gamma_{LCO_2} = 10^{-3} (b_{00} + b_{10}P + b_{01}T + b_{20}P^2 + b_{11}PT + b_{02}T^2 + b_{30}P^3 + b_{21}P^2T + b_{12}PT^2 + b_{40}P^4 + b_{31}P^3T + b_{22}P^2T^2) \quad (4.25)$$

$$\gamma_{LH_2} = 10^{-3} (b_{00} + b_{10}P + b_{01}T + b_{20}P^2 + b_{11}PT + b_{02}T^2 + b_{30}P^3 + b_{21}P^2T + b_{12}PT^2 + b_{03}T^3 + b_{40}P^4 + b_{31}P^3T + b_{22}P^2T^2 + b_{13}PT^3 + b_{50}P^5 + b_{41}P^4T + b_{32}P^3T^2 + b_{23}P^2T^3) \quad (4.26)$$

Biogas bubble specie velocity in the liquid phase, dh_{j_*}/dt (m.s⁻¹)

$$\frac{dh_{j_*}}{dt} \cong u_b \cong \frac{\rho_L g d_{j_*}^2}{27\eta_L} \quad (4.27)$$

Dynamics of moles of biogas bubble species, dn_{bj_*}/dt (kgmole.s⁻¹)

$$\frac{dn_{bj_*}}{dt} = \frac{\pi d_{j_*}^2 K_{Lj_*} (G_{Dj_*} - K_{Hj_*} p_{j_*})}{M_{j_*}} \quad (4.28)$$

Estimation of film coefficient of biogas species, K_{Lj_*} (m.s⁻¹)

$$\frac{K_{Lj_*} (2r_{Ri})}{D_{Lj_*}} = 0.322 N_{Re}^{0.7} Sc^{1/3} \quad (4.29)$$

Where Schmidt number, $Sc = \eta_L / \rho_L D_{Lj_*}$ and Reynold number of mixing,

$$N_{Re} = \rho_L n_{st} d_{st}^2 / \eta_L$$

Estimation of bubble size distribution, $f(d_{j_*h})$

$$f(d_{j_*h}) = \frac{1}{\zeta_* \sqrt{2\pi}} \exp \left\{ -\frac{1}{2} \left(\frac{d_{j_*h} - d_{j_*m}}{\zeta_*} \right)^2 \right\} \quad (4.30a)$$

$$\zeta_* = \sqrt{\sum_{h=1}^H (d_{j_*h} - d_{sj_*})^2 / H} \quad (4.30b)$$

$$d_{sj_*} \cong \frac{\sum_{h=1}^H d_{j_*h}^3}{\sum_{h=1}^H d_{j_*h}^2} \quad (4.30c)$$

$d_{j_*m} \cong d_{sj_*}$ and d_{j_*h} is diameter of each time steps, $h = 1, 2, \dots, H$

Biogas outflow rate, q_{o-G} (m³.s⁻¹)

$$q_{o-G} = k_p (P_G + P_{sw} - P_R) ((P_G + P_{sw}) / P_R) \quad (4.31)$$

Dynamics of ion concentration, $d[Z]/dt$ (kgmoles.m⁻³.s⁻¹)

$$\frac{d[Z]}{dt} = \frac{q_{i-L}}{V_L} ([Z]_i - [Z]) + \frac{q_{c-L}}{V_L} ([Z_c] - [Z]) \quad (4.32a)$$

$$+ \frac{[Z]}{\rho_L} \left(R_{E-G} + \frac{R_{Evap}}{V_L} + q_{o-GG} W_{H_2O} \right) + R_Z \quad (4.32b)$$

$$R_Z \cong Y_{cat} (\mu_1 + \mu_2) / M_B$$

pH of the bioreactor

$$pH = -\log_{10}[H^+] \quad (4.33a)$$

$$\frac{d[H^+]}{dt} = \frac{K_{aCO_2}}{[HCO_3^-]M_{CO_2}} \frac{dG_{DCO_2}}{dt} \quad (4.33b)$$

$$[HCO_3^-] = [Z] - [Ac^-] \quad (4.33c)$$

$$[Ac^-] = \frac{Ac[H^+]}{M_{Ac}K_{aAc}} \quad (4.33d)$$

$$K_{aj\pm} = \exp\left\{\frac{\Delta v_{j\pm} \psi_{j\pm}^{0\pm}}{0.0821T}\right\} \quad (4.33e)$$

Dynamics of bioreactor temperature, dT/dt ($K.s^{-1}$)

$$\frac{dT}{dt} = \frac{1}{(V_L \rho_L C_{pL} + V_G G C_{pG} + V_G W_V C_{pW_V})} [q_{i-L} \rho_L C_{pL} (T_i - T) + q_{c-L} \rho_L C_{pL} (T_c - T) + q_{o-GG} W_{H_2O} (C_{pL} - C_{pW_V}) T + R_{Evap} (C_{pL} - C_{pW_V}) T + V_L R_{E-G} (C_{pL} - C_{pG}) T + V_L R_{AD} \Delta H_{AD} - (R_{Evap} + q_{o-GG} W_{H_2O}) \Delta H_{Evap} + (Q_{HE} + P_{Mix} - Q_{R-En})] \quad (4.34a)$$

$$R_{AD} = \sum_j \frac{1}{Y_{S_j/F}} \left(\frac{\mu_j B_j}{Y_{B_j/S_j}} \right) = \frac{1}{Y_{S_1/F}} \left(\frac{\mu_1 B}{Y_{B/S_1}} \right) + \frac{1}{Y_{S_2/F}} \left(\frac{\mu_2 B}{Y_{B/S_2}} \right) \quad (4.34b)$$

$$\frac{Q_{HE}}{A_{Ro}} = U_{HE-o} (T_{hw} - T) = \bar{h}_{Hi} (T_{wh} - T) = \frac{Q_{HE}}{A_R} = \frac{\bar{h}_R (T_{wh} - T_{wc})}{x_R} \quad (4.34c)$$

$$U_{HE-o} = \frac{1}{\frac{1}{\bar{h}_H} + \frac{x_R}{\bar{h}_R} \left(\frac{D_o}{\bar{D}} \right) + \frac{1}{\bar{h}_R} \left(\frac{D_o}{D_i} \right)} \quad (4.34d)$$

$$\bar{D}_R = (D_{Ro} - D_{Ri}) \ln(D_{Ro}/D_{Ri}) \quad (4.34e)$$

Power of the mixer (W)

$$P_{Mix} = N_p \eta_L n_{st}^2 d_{st}^3 \text{ or } P_{Mix} = N_p \rho_L n_{st}^3 d_{st}^5 \quad (4.35)$$

Dynamics of heating jacket temperature ($K.s^{-1}$)

$$\frac{dT_{hw}}{dt} = \frac{q_{hw} (T_{i-hw} - T_{hw})}{V_{hw}} - \frac{(Q_{HE} + Q_{H-En})}{\rho_{hw} V_{hw} C_{p-hw}} \quad (4.36a)$$

$$\begin{aligned} \frac{Q_{H-En}}{A_{H-i}} &= U_{H-Eni} (T_{hw} - T_{Air}) = \bar{h}_{Ho} (T_{hw} - T_{H-wh}) = \frac{Q_{H-En}}{A_H} \\ &= \frac{\bar{h}_H (T_{H-wh} - T_{H-wc})}{x_{Ho}} \end{aligned} \quad (4.36b)$$

$$U_{H-Eni} = \frac{1}{\frac{1}{\bar{h}_{Ho}} + \frac{x_{Ho}}{\bar{h}_{Ho}} \left(\frac{D_{H-i}}{\bar{D}_H} \right) + \frac{1}{\bar{h}_{Air}} \left(\frac{D_{H-i}}{D_{H-o}} \right)} \quad (4.36c)$$

$$\bar{D}_H = (D_{H-o} - D_{H-i}) \ln(D_{H-o}/D_{H-i}) \quad (4.36d)$$

Heat transfer coefficient for the bioreactor, \bar{h}_R ($W.m^{-2}.K^{-1}$)

$$\bar{h}_R = \sqrt[4]{\bar{h}_L^4 + \bar{h}_G^4} \quad (4.37a)$$

$$\text{Nu} = \left(\frac{\dot{h}_j L_c}{k_j} = \Theta_1 N_{\text{Re}}^{2/3} \text{Pr}^{1/3} \left(\frac{\eta_j}{\eta_{\text{wj}}} \right)^{\Theta_2} \right)_{j=\text{L}} \quad (4.37\text{b})$$

$$\text{Nu} = \left(\frac{\dot{h}_j L_c}{k_j} = \left(0.825 + \frac{0.387(\text{GrPr})^{1/6}}{(1 + (0.492/\text{pr})^{9/16})^{8/27}} \right)^2 \right)_{j=\text{G}} \quad (4.37\text{c})$$

Heat transfer coefficient for the bioreactor, \dot{h}_{Hi} (W.m⁻².K⁻¹)

$$\text{Nu} = \left(\frac{\dot{h}_j L_c}{k_j} = \left\{ 3.66 + \frac{0.065 \text{RePr} D_{\text{H-i}}/h_{\text{R}}}{1 + 0.04(\text{RePr} D_{\text{H-i}}/h_{\text{R}})^{2/3}} \right\} \left(\frac{\eta_j}{\eta_{\text{wj}}} \right)^{0.11} \right)_{j=\text{Hi}} \quad (4.38\text{a})$$

$$\text{Nu} = \left(\frac{\dot{h}_j L_c}{k_j} = 0.0243 \text{Re}^{0.8} \text{Pr}^{0.3} \left(\frac{\eta_j}{\eta_{\text{wj}}} \right)^{0.14} \right)_{j=\text{Hi}} \quad (4.38\text{b})$$

$N_{\text{Re}} = \rho_j n_{\text{st}} d_{\text{st}}^2 / \eta_j$, $\text{Pr} = C_{\text{p}j} \eta_j / k_{\text{L}}$, $\text{Gr} = g \beta \rho_j^2 |\Delta T| L_c^3 / \eta_j$, $\beta = \Delta \rho_j / (\rho_{\text{av}j} \Delta T)$
or $\beta \cong 1/T_f$ as well as $\Theta_1 = 0.36$ and $\Theta_2 = 0.21$.

Table 4.1. Coefficients of the polynomial model used for the calculation of the interfacial tension.

Coefficients, b_{ij}	Values, γ_{LCO_2}	Values, γ_{LH_2}
b_{00}	19.3506	-95.7078
b_{10}	-67.5188	14.9137
b_{01}	0.4142	1.5894
b_{20}	4.4881	-0.4375
b_{11}	0.3091	-0.1203
b_{02}	-0.0008	-0.0046
b_{30}	-0.0392	0.0056
b_{21}	-0.0202	0.0028
b_{12}	-0.0004	0.0003
b_{03}	–	3.95E-06
b_{40}	0.0001	-9.89E-05
b_{31}	8.17E-05	-9.43E-06
b_{22}	2.38E-05	-7.07E-06
b_{13}	–	-3.03E-07
b_{50}	–	2.26E-07
b_{41}	–	2.05E-07
b_{32}	–	-8.93E-09
b_{23}	–	6.75E-09

4.1. Experimental analysis of lipid hydrolysis

The kinetic constant, K_{lipid} , for lipid hydrolysis, Equation (6.4f), is deduced experimentally and modelled as a function of temperature.

5. Experimental framework – Materials and methods

5.1. Collection and storage of sludge sample

A substantial amount of industrial-activated sludge sample was sourced from a biogas production plant. The sample was filtered to enhance its homogeneity, its properties measured, Table (5.1), and stored in a refrigerator at 4 °C to minimise its activity.

Table 5.1. Average physicochemical properties, and composition of sludge sample

Properties, unit	Results
pH, 19.7°C	7.3200±0.0016
Density, 20 °C H ₂ O	0.9900±0.0002
Total suspended solids (TSS), kg.m ⁻³	22.391±3.5910
Volatile suspended solids (VSS), kg.m ⁻³	13.459±0.5220
Biochemical oxygen demand (BOD), kg.m ⁻³	1.5700±0.1500
Chemical oxygen demand (COD), kg.m ⁻³	21.300±0.1500
Total kjeldahl nitrogen (TKN), kg.m ⁻³	0.5660±0.1500
Triglyceride, kg.m ⁻³	0.0105±0.0050
Diglyceride, kg.m ⁻³	0.0102±0.0050
Monoglyceride, kg.m ⁻³	0.1194±0.0050
LCFA, kg.m ⁻³	0.0918±0.0050

5.2. Dispersion of lipid sample in sludge

To standardise the procedure of monitoring lipid hydrolysis, a known amount of lipid (specifically, rapeseed oil) is added to the sludge sample. Considering the low solubility and consequently inhomogeneity of lipids in aqueous solutions, the lipid was emulsified and stabilised using xanthan gum. In the presence of a continuous flow of nitrogen, 130 g of stored sludge placed in a beaker was stirred at 2000 rpm in a temperature-controlled stirrer to 25, 30, 35, 45, and 50 °C. At each condition, 0.33 g (i.e., 2.5 kg.m⁻³ of lipid) of lipid was slowly added, while stirring continued for 15 minutes. Furthermore, 0.33 g of xanthan gum powder was slowly added with stirring for another 15 minutes before the process was stopped.

5.3. Setup of the anaerobic hydrolysis system

The prepared oil-sludge emulsion was then transferred to a 250 mL Fisherbrand glass reactor (FB-800-250) and placed in a temperature-controlled water bath (Mettler, WNB 22) with an inbuilt shaking device. The reactor was stirred horizontally at 160 strokes per minute and each temperature (i.e., 25, 30, 35, 45, and

50 °C). Finally, to monitor the hydrolysis kinetics, samples were collected from the reactor periodically (i.e., 0.00, 0.50, 1.00, ..., 24.0 hours) in the presence of nitrogen.

5.4. Analysis of hydrolysed lipid

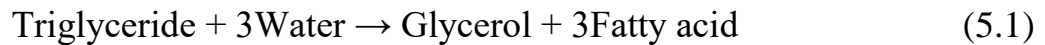
The qualitative and quantitative analysis of lipid hydrolysis was performed using gas chromatography (GC). In the GC analysis, 0.2 g of samples in duplicate were withdrawn from the reactor periodically as described by Šánek et al. [24].



Figure 5.1. Experimental setup utilised for the anaerobic digestion

5.5. Modelling lipid hydrolysis kinetics

The reaction kinetics, R_F of the lipid feedstock (i.e., triglyceride = F) in the sludge was investigated using the generic single-step first-order kinetic model, Equation (5.2). In Equation (5.2), it is assumed the rate constants, k_{Lipid} is temperature dependent, as such can be modelled by the 1st term Gaussian model, Equation (5.3).



$$R_F = dF/dt = -k_{Lipid}F \quad (5.2)$$

$$k = k_0 e^{-\left(\frac{T-T_0}{K_T}\right)^2} \quad (5.3)$$

Where $T(K)$ is the reaction temperature, $T_0(K)$ is the reference temperature, $k_0(\text{hr}^{-1})$ is the preexponential factor of the reaction, and $k_T(K^{-1})$ is a temperature constant. The curve-fitting procedure can be implemented in MATLAB through the `Lsqcurvefit` function and the `ode45` numerical non-stiff solver.

5.6. Evaluation of models

The accuracy or evaluation metrics for the proposed kinetic models, as do other curve-fitted models in this work can be checked using R-squared (R^2) value, Equation (5.4). Where y is the output, \bar{y} is the mean output of the data set, and \hat{y} is model output.

$$R^2 = 1 - \frac{\Sigma(y - \hat{y})^2}{\Sigma(y - \bar{y})^2} \quad (5.4)$$

5.7. Simulation of model

The Equations (4.1) – (4.38) of develop dynamic models as well as analytical/empirical models together with Equation (A.41) – (A.44) were solved using ODE15s (a stiff numerical solver) as well as lsqnonlin function (an iterative estimation of the bioreactor and heating jacketing wall temperature) in MATLAB via data in Table (3.1), (4.1), (5.2), (6.1), and (6.2), including the thermochemical properties of components given in Equation (A.1) – (A.38) of the Appendix section.

Table 5.2. Simulation parameters based on laboratory scale, and literature review

Symbols	Description	Values (units)
r_{Ri} and r_{Ro}	Inner and outer radius of Bioreactor (BR)	0.0300 and 0.0307 m
r_{Hi} and r_{Ho}	Hydraulic radius of heating jacket (HJ)	0.01 and 0.0107 m
h_R	Total height of BR=HJ	0.218 m
h_L	Liquid level in BR	0.082 m
q_{i-L} and q_{o-L}	Inflow and outflow rate of liquid in the BR	$0 \text{ m}^3 \cdot \text{hr}^{-1}$
q_{c-L}	pH inflow rate	$0 \text{ m}^3 \cdot \text{hr}^{-1}$
g & R	Acceleration due to gravity & Ideal gas constant	$9.81 \text{ m} \cdot \text{s}^{-2}$ & $8314 \text{ J} \cdot \text{kgmol}^{-1} \cdot \text{K}^{-1}$
F	Initial concentration of lipid	$2.5385 \text{ kg} \cdot \text{m}^{-3}$
B	Initial concentration of microbes	$0.01 \text{ kg} \cdot \text{m}^{-3}$
$[Z]$	Molar concentration of artificial ion	$0.00035 \text{ kgmoles} \cdot \text{m}^{-3}$
$[Z_c]$	pH controller artificial ion	$0.000 \text{ kgmoles} \cdot \text{m}^{-3}$
T and T_{hw}	Initial temperature of fluid in BR, and HJ	35 and 60 °C
T_{Air}	Environment or surround air temperature	25 °C
Φ_v	Volatile fraction of the feedstock	$\Phi_G = 0.9$ and $\Phi_B = 0.1$
pH	Initial pH of BR	8.23
Y_{cat}	Cation yield from microbes	1.000

\bar{i}_{pH-j*}	Ideal inhibition of various biogas species	$\bar{i}_{pH-j*} = 1$
pH_{ll}	Lower pH limit for CH ₄ , CO ₂ , and H ₂	6.5, 5.0, and 5.0
pH_{ul}	Upper pH limit for CH ₄ , CO ₂ , and H ₂	7.5, 7.5, and 7.5
$-(\Delta\psi_{j*}^{ovl})$	Chemical potential difference for CH ₄ , CO ₂ , and H ₂	158.084, 75.4238, and 172.7239
$\Delta v_{j\pm} \psi_{j\pm}^{o\pm}$	Summation of chemical ion potentials for HCO ₃ ⁻ and acetic acid	-358.8272, and -267.9815
$(K_L a)_{H_2}$	Hydrogen gas-liquid mass transfer coefficient	0.0027 s ⁻¹
K_{d-1} & K_{d-2}	Death rate for microbes in substrate (1) and (2)	$K_d=0.05\mu_{max}$
K_{S_1} & K_{S_2}	Half-saturation coefficient for substrate (1) and (2)	3.18 & 1.00 kg.m ⁻³
K_p	Pipe resistance coefficient	0.000001 Pa.m ³ .hr ⁻¹
d_{j*}	Initial bubble diameter	0.00050 m
ΔH_{AD}	Heat of reaction of the anaerobic	0.0690 kJ.g ⁻¹
N_p	Power number of the bioreactor stirrer	0.309
n_{st}	Stirrer speed	100 rpm
d_{st}	Diameter of stirrer	0.65(2r _{Ri})

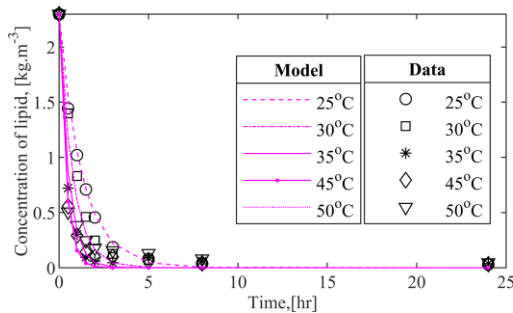
6. Results

6.1. Hydrolysis kinetics

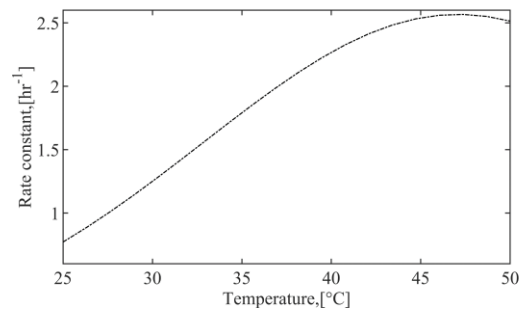
Evaluation of the developed kinetic model with experimental data given in Table (A.3) of the Appendix section, indicates a significant fit as shown in Figure (6.1), and Table (6.1) with an average $R^2 = 0.9895$.

Table 6.1. Hydrolysis model based on the single-step curve-fitting methods.

	Gaussian model constants				
	k_0, h^{-1}		k_T, K^{-1}		T_0, K
	2.5667		20.1518		320.0911
	Temperature, °C				
	25	30	35	45	50
k_{Lipid}, hr^{-1}	0.7717	1.2502	1.7907	2.5392	2.5138
R^2	0.9964	0.9901	0.9912	0.9942	0.9756



a. Model and experimental comparison



b. Gaussian thermodynamic model

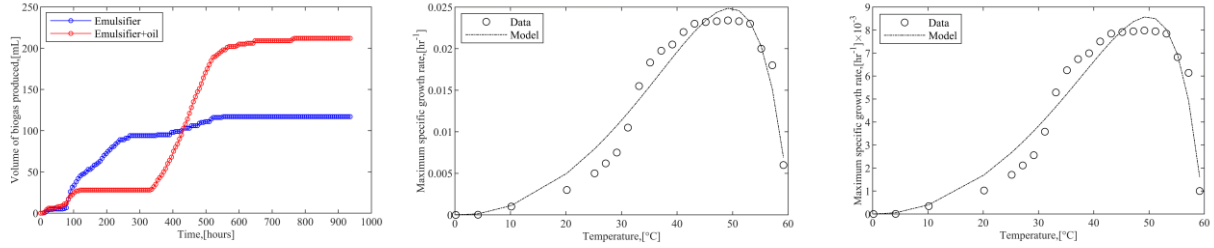
Figure 6.1. Illustration of hydrolysis kinetic, and Gaussian model for lipid degradation

The resulting biogas production for the oil-sludge emulsion at 35 °C beyond the time limit of lipid hydrolysis is also illustrated in Figure (6.2a). The methane and carbon dioxide volumetric content in the produced biogas were respectively found cumulatively (i.e., at the end of the biogas production process) to be about 62% and 38% using the methodology developed via FTIR.

Furthermore, the Ratkowsky model, Equation (4.6c), was applied to theoretically approximate the maximum microbe specific growth rate, μ_{max} . The model was curve-fitted based on hypothetical data for LCFA and glycerol, as illustrated in Table (6.2) and Figure (6.2b) – (6.2c).

Table 6.2. Ratkowsky constants for estimation of maximum specific growth rate

Substrate/parameter	R^2	$\mathcal{B}_1(K^{-1}.h^{-1/2})$	$\mathcal{B}_2(K^{-1})$	$T_{min}(K)$	$T_{max}(K)$
LCFA	0.9571	0.0037	0.1331	274.1496	333.3498
Glycerol	0.9525	0.0021	0.1558	273.6860	332.8614



a. Biogas production *b. LCFA microbe activity* *c. Glycerol microbe activity*
Figure 6.2. Biogas production, and maximum microbe specific growth rate

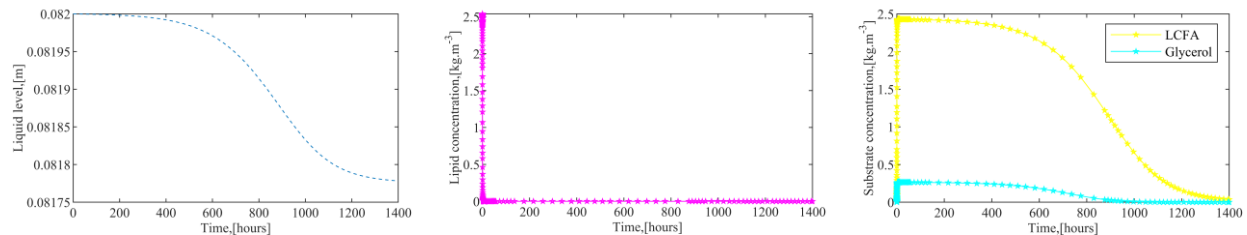
6.2. Anaerobic digestion simulation

6.2.1. Effect of pressure

To elaborate on the effect of pressure, the developed SSDM model was simulated for three (3) case studies at 35 °C (i.e., heating water flowrate, $q_{hw} = 0.0000000040 \text{ m}^3.s^{-1}$), and negligible pH inhibition. These case studies include Case-study-A(P) (Complete batch system without output of biogas, i.e., overpressure), Case-study-B(P) (Semi-batch system with output of biogas at atmospheric pressure), and Case-study-C(P) (Semi-batch system with output of biogas below atmospheric pressure, typically 30% atmospheric pressure). The bioreactor is assumed initialised with nitrogen-inert gas at atmospheric pressure (101325 pa). The inert concentration and corresponding pressure in the headspace are modelled using Equation (4.9) but with $R_{E-j*} = 0$, and the ideal gas law equation respectively.

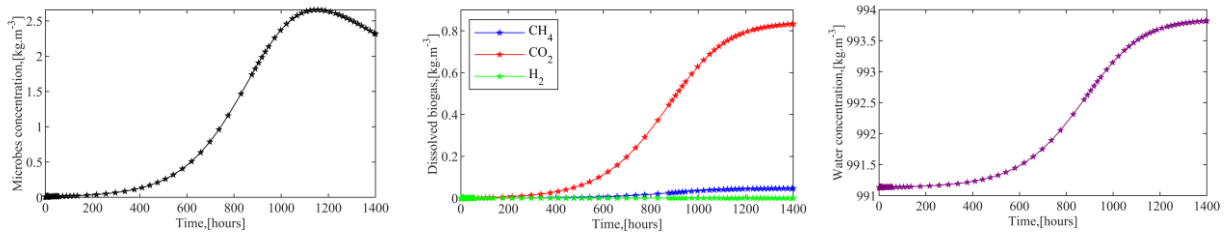
Case-study-A(P)

Case-study-A(P) considers a complete batch system without output of biogas, i.e., $q_{0-G} = 0$.



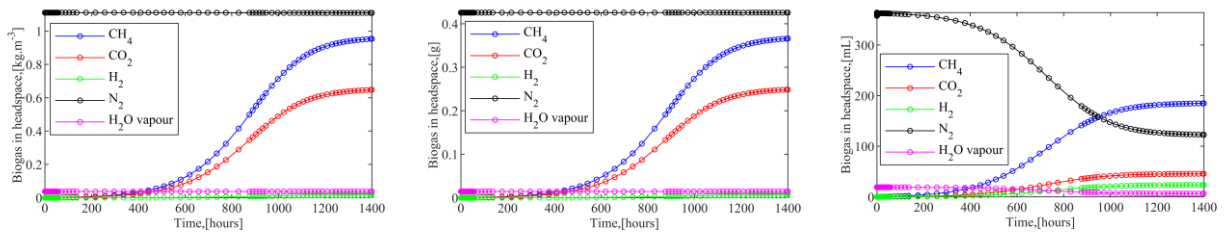
a. Level dynamics *b. Lipid dynamics* *c. Substrate dynamics*

Figure 6.3. Changes in liquid level, lipid, and microbes in the liquid phase (1)



a. Microbes' dynamics b. Dissolved gas dynamics c. Dynamics of water

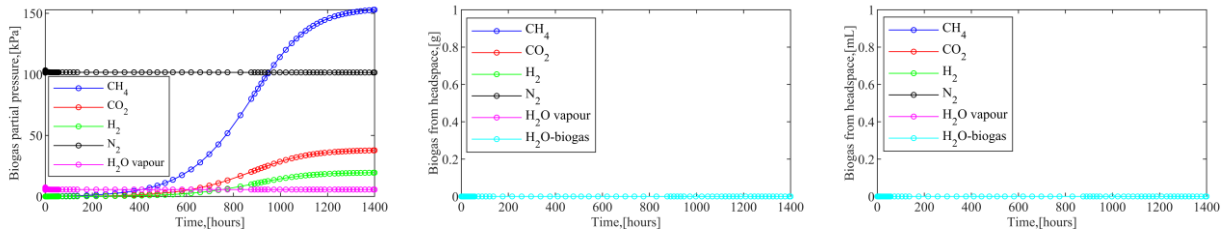
Figure 6.4. Concentration dynamics for microbes, biogas formation and water (1)



a. Concentration of biogas b. Mass of biogas c. Volume of biogas

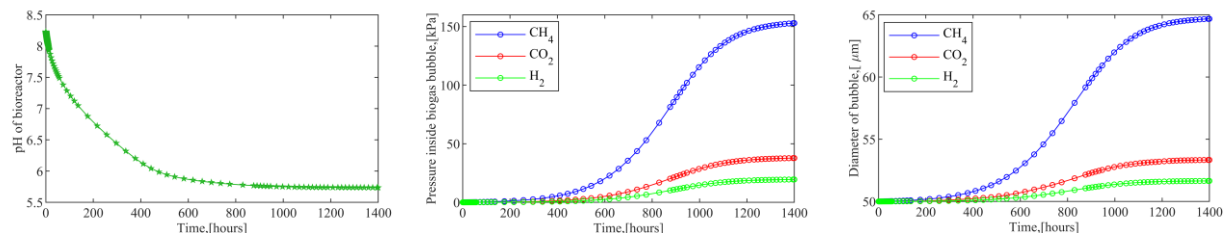
Figure 6.5. Concentration, mass, and volume of biogas obtainable in headspace (1)

* H_2O vapour and H_2O -biogas respectively indicate water vapour and inherent biogas water



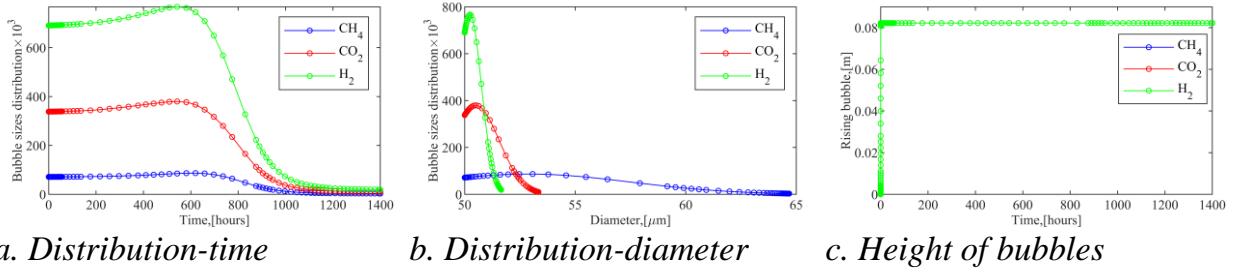
a. Headspace pressure b. Mass of biogas c. Volume of biogas

Figure 6.6. Pressure in headspace, mass, and volume of biogas from headspace (1)

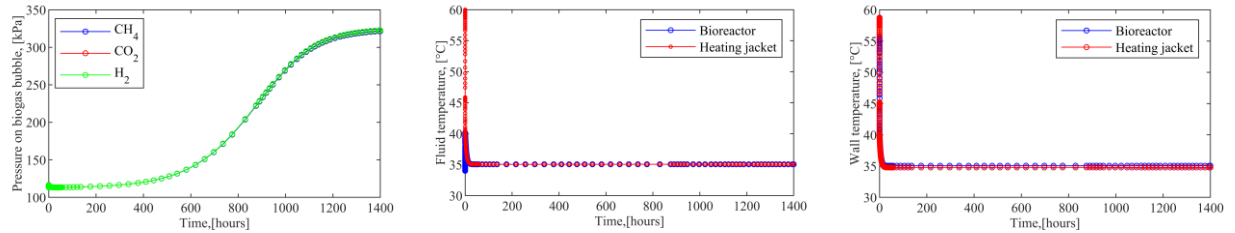


a. pH of bioreactor b. Pressure in bubbles c. Diameter of bubbles

Figure 6.7. pH bioreactor, pressure in bubbles, and diameter of biogas bubbles (1)



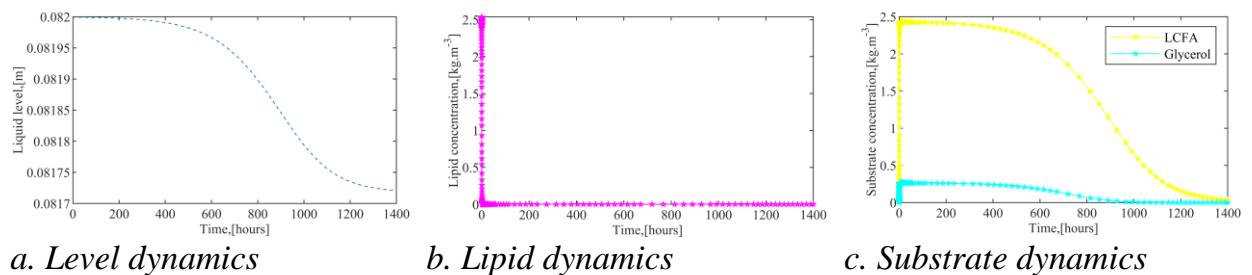
a. Distribution-time b. Distribution-diameter c. Height of bubbles
Figure 6.8. Biogas bubbles distribution and its rising height in liquid phase (1)



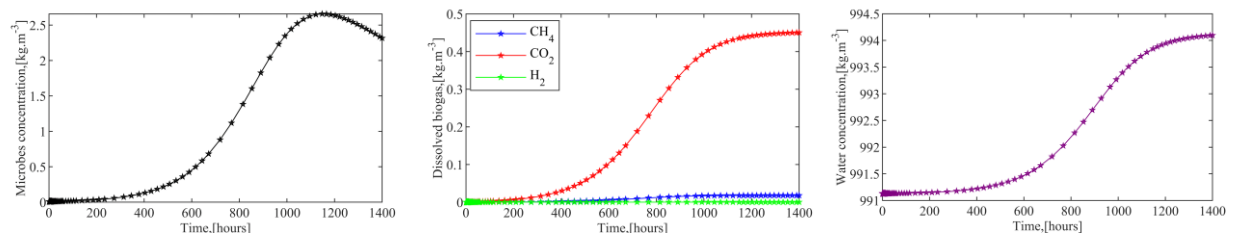
a. Pressure on bubbles b. Fluid temperatures c. Wall temperatures
Figure 6.9. Bubbles surface pressure, fluid, and wall temperature of reaction system (1)

Case-study-B(P)

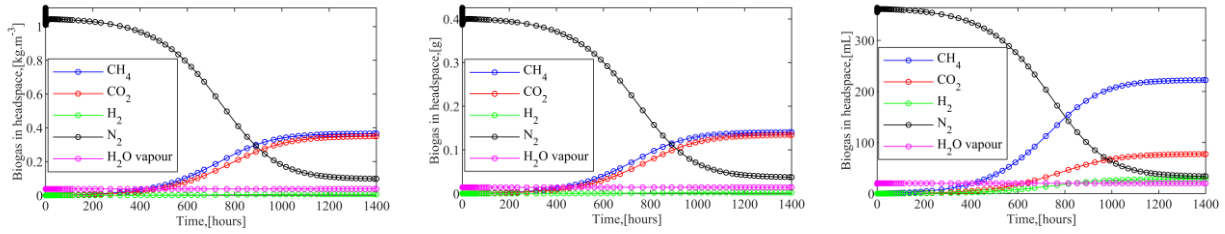
Case-study-B(P) is a semi-batch reactor, whose biogas outflow, q_{o-G} , is regulated by the total pressure of the gas headspace as given by Equation (6.16). The bioreactor is assumed to operate at atmospheric pressure like the experimental condition considered in this work.



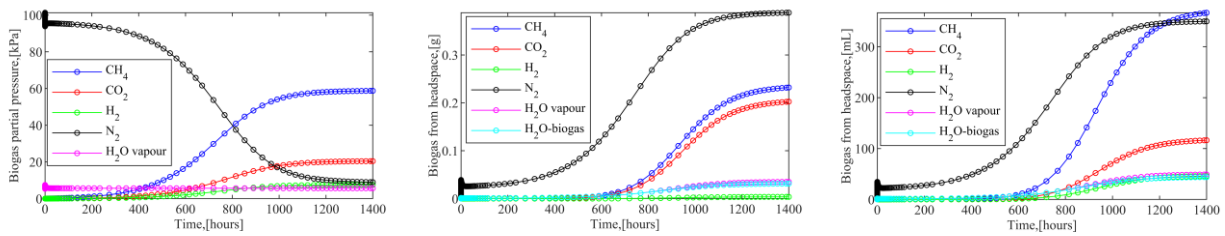
a. Level dynamics b. Lipid dynamics c. Substrate dynamics
Figure 6.10. Changes in liquid level, lipid, and microbes in the liquid phase (2)



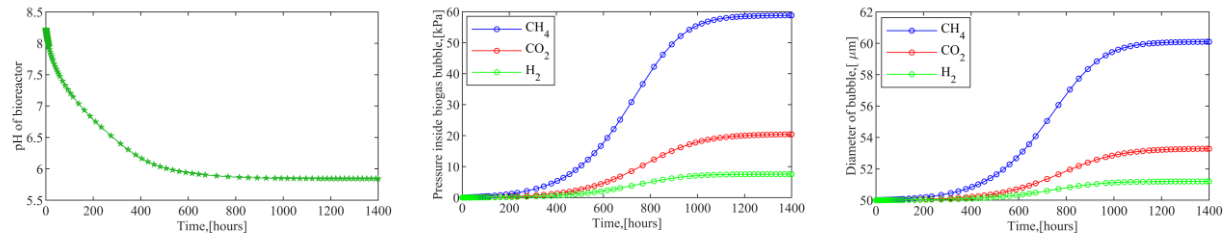
a. Microbes' dynamics b. Dissolved gas dynamics c. Dynamics of water
Figure 6.11. Concentration dynamics for microbes, biogas formation and water (2)



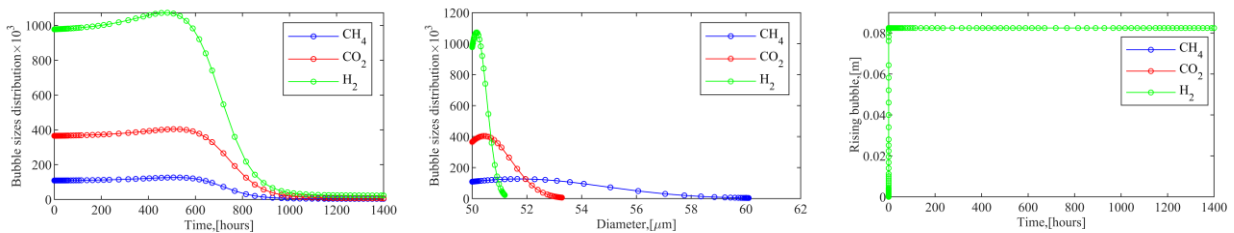
a. Concentration of biogas b. Mass of biogas c. Volume of biogas
Figure 6.12. Concentration, mass, and volume of biogas obtainable in headspace (2)



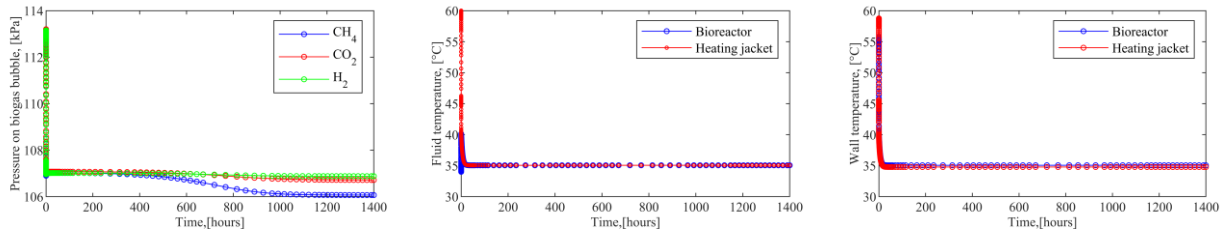
a. Headspace pressure b. Mass of biogas c. Volume of biogas
Figure 6.13. Pressure in headspace, mass, and volume of biogas from headspace (2)



a. pH of bioreactor b. Pressure in bubbles c. Diameter of bubbles
Figure 6.14. pH bioreactor, pressure in bubbles, and diameter of biogas bubbles (2)



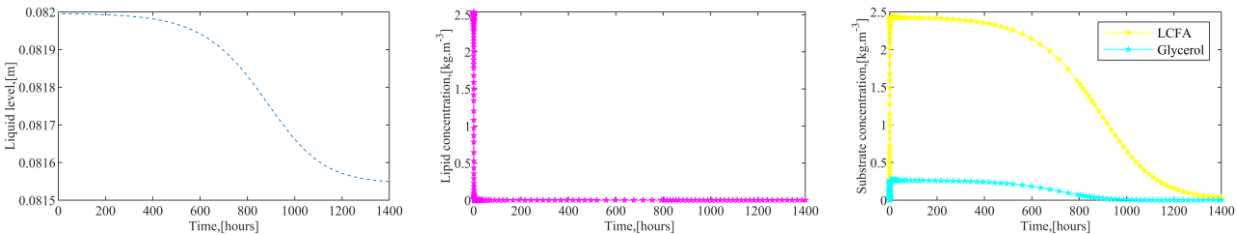
a. Distribution-time b. Distribution-diameter c. Height of bubbles
Figure 6.15. Biogas bubbles distribution and its rising height in liquid phase (2)



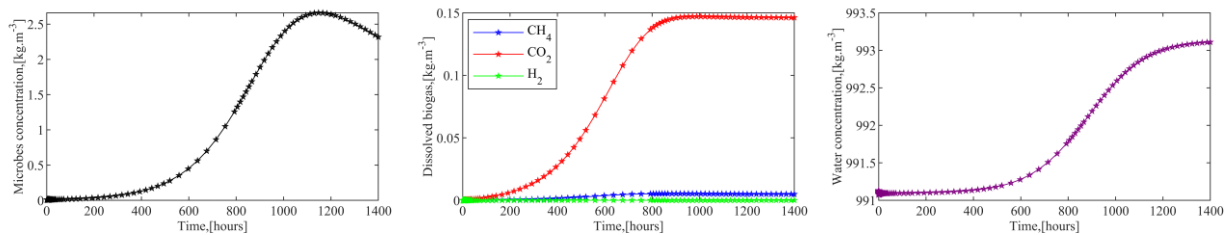
a. Pressure on bubbles b. Fluid temperatures c. Wall temperatures
Figure 6.16. Bubbles surface pressure, fluid, and wall temperature of reaction system (2)

Case-study C(P)

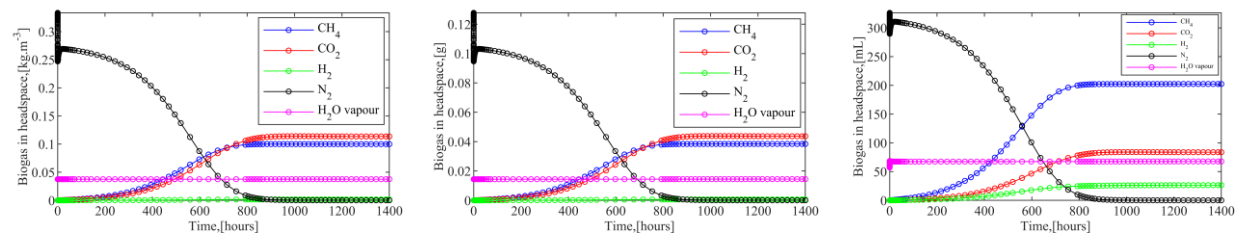
Case-study-C(P) is also a semi-batch reactor. However, in this case, the bioreactor is assumed to operate at some vacuum, specifically 30% atmospheric pressure. Although this case study might not be practicable commercially, and expensive to operate, the essence of this simulation is to evaluate the robustness of the model, as well as further elucidate the effect of pressure.



a. Level dynamics b. Lipid dynamics c. Substrate dynamics
Figure 6.17. Changes in liquid level, lipid, and microbes in the liquid phase (3)



a. Microbes' dynamics b. Dissolved gas dynamics c. Dynamics of water
Figure 6.18. Concentration dynamics for microbes, biogas formation and water (3)



a. Concentration of biogas b. Mass of biogas c. Volume of biogas

Figure 6.19. Concentration, mass, and volume of biogas obtainable in headspace (3)

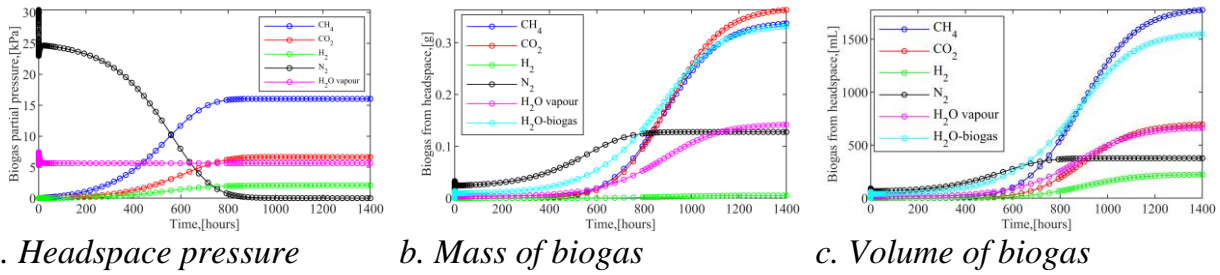


Figure 6.20. Pressure in headspace, mass, and volume of biogas from headspace (3)

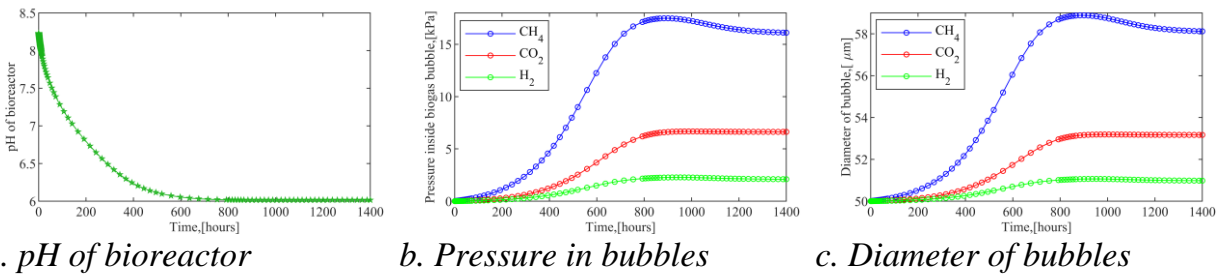


Figure 6.21. pH bioreactor, pressure in bubbles, and diameter of biogas bubbles (3)

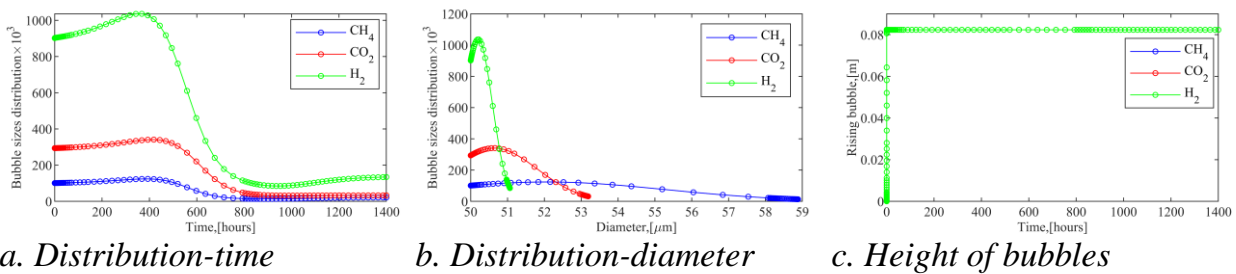


Figure 6.22. Biogas bubbles distribution and its rising height in liquid phase (3)

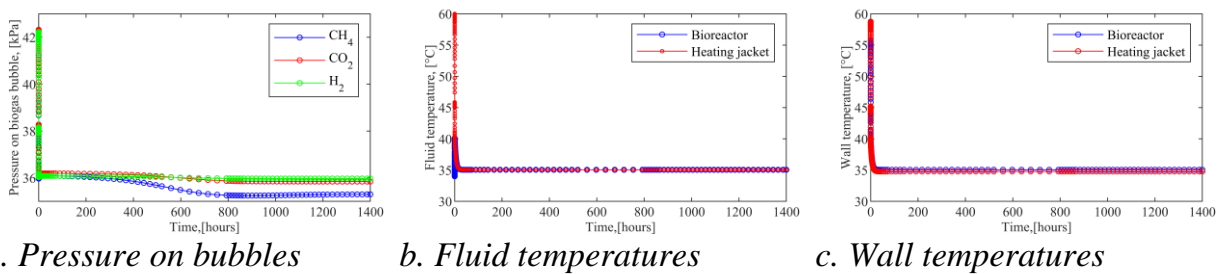


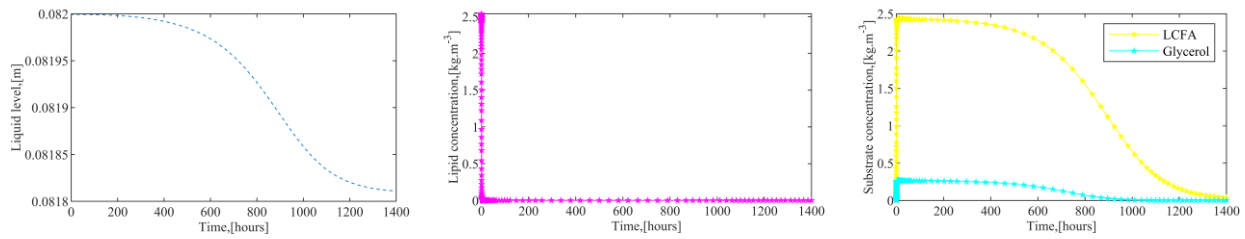
Figure 6.23. Bubbles surface pressure, fluid, and wall temperature of reaction system (3)

In summary of the effect of pressure on AD, it can be inferred that operating the AD process at higher pressure enhances the solubility of the carbon dioxide in the liquid

phase. Thus, resulting to a higher proportion of methane gas in the headspace, but at the expense of lowering the pH of the system due to higher dissolved carbon dioxide. Regarding biogas bubble growth, higher pressure leads to larger biogas bubbles, which correspondingly limit the bubble size distribution in the system.

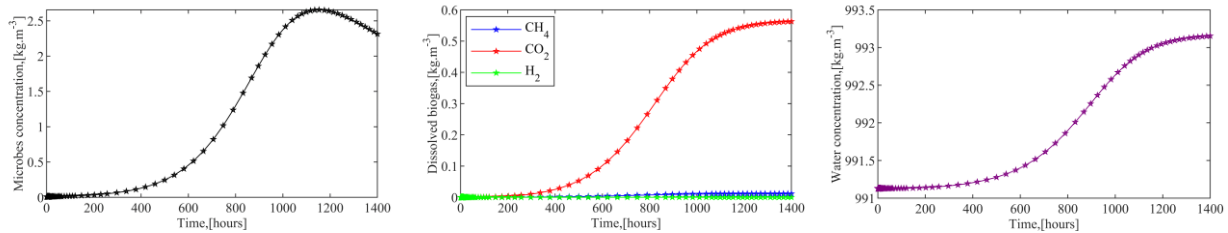
6.2.2. Effect of pH inhibition

Considering that the Case-study-B(P) is the exact experimental condition applied in this work, therefore its conditions (i.e., 35 °C, and 101325 Pa) are applied to illustrate the effect of pH inhibition on the AD process.



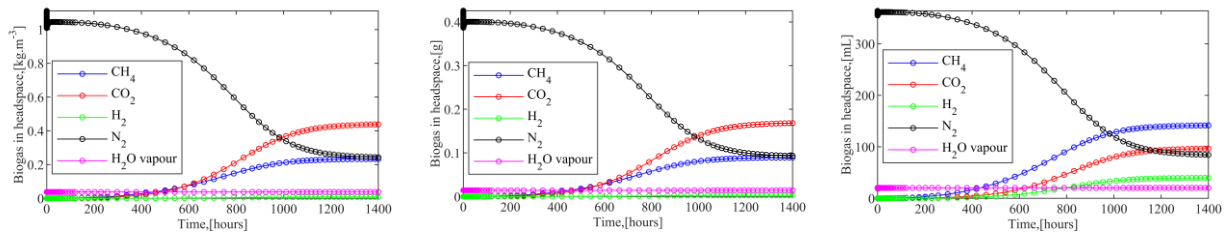
a. Level dynamics b. Lipid dynamics c. Substrate dynamics

Figure 6.24. Changes in liquid level, lipid, and microbes in the liquid phase (4)



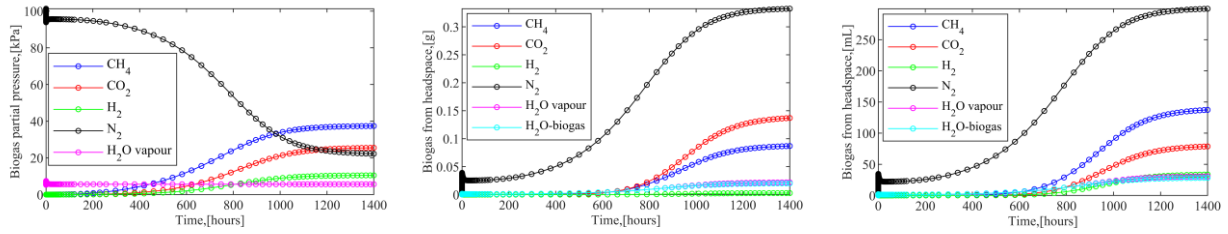
a. Microbes' dynamics b. Dissolved gas dynamics c. Dynamics of water

Figure 6.25. Concentration dynamics for microbes, biogas formation and water (4)

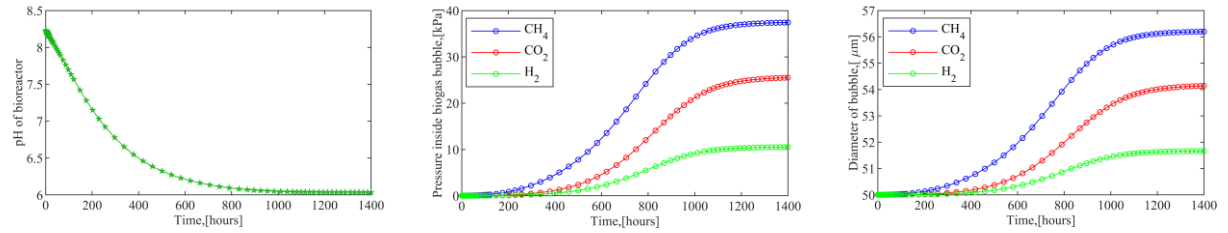


a. Concentration of biogas b. Mass of biogas c. Volume of biogas

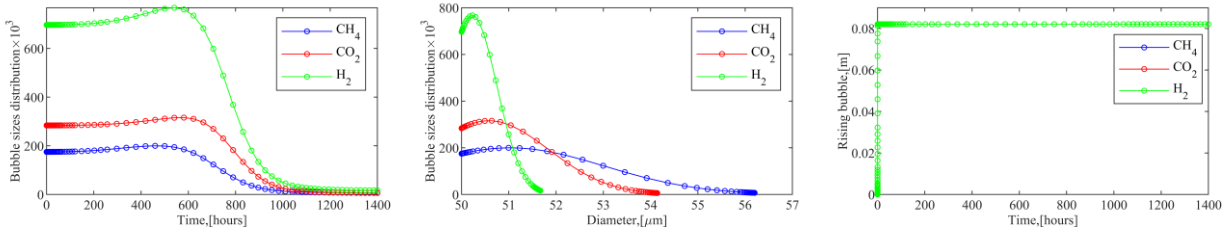
Figure 6.26. Concentration, mass, and volume of biogas obtainable in headspace (4)



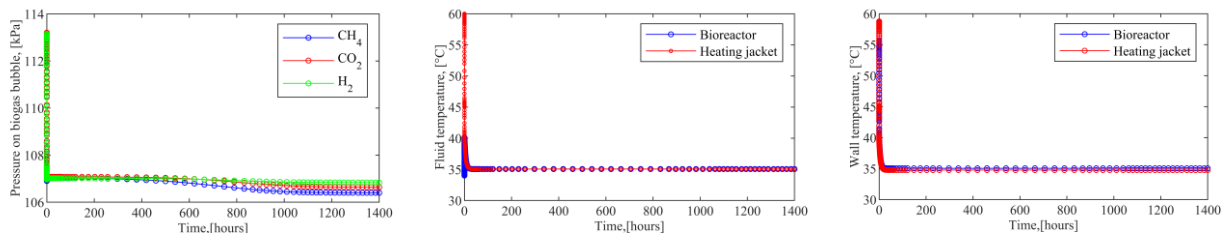
a. Headspace pressure b. Mass of biogas c. Volume of biogas
Figure 6.27. Pressure in headspace, mass, and volume of biogas from headspace (4)



a. pH of bioreactor b. Pressure in bubbles c. Diameter of bubbles
Figure 6.28. pH bioreactor, pressure in bubbles, and diameter of biogas bubbles (4)



a. Distribution-time b. Distribution-diameter c. Height of bubbles
Figure 6.29. Biogas bubbles distribution and its rising height in liquid phase (4)



a. Pressure on bubbles b. Fluid temperatures c. Wall temperatures
Figure 6.30. Bubbles surface pressure, fluid, and wall temperature of reaction system (4)

Comparing the amount of biogas produced experimentally (230 mL) to that simulated in this case study (575 mL). This implies that the anaerobic digestion process proceeded only by about 40%, which is not too far off the reported percentage conversion of AD, i.e., about 49.97% [25].

In summary, regarding the pH inhibition, considering that methanogenesis operates at higher pH conditions (i.e., close to neutral pH). Methane production is, therefore, more inhibited in the bioreactor, especially since the simulated pH is between 5.6 – 6.0 approximately. Therefore, with the limitation of biogas production, the biogas bubble growth as well as its size distribution is limited.

6.2.3. Effect of temperature

Case-study-A(T)

This case study focuses on applying atmospheric pressure to investigate the effect of temperature on the AD process, the conditions of Case-study-B(P) are applied based on earlier reasons. The temperature of the system is increased to 45 °C (i.e., based on heating water flowrate, $q_{hw} = 0.0000000158 \text{ m}^3 \cdot \text{s}^{-1}$).

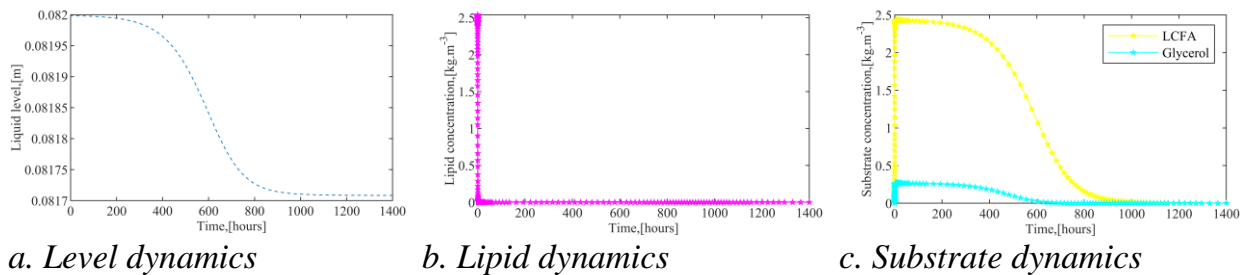


Figure 6.31. Changes in liquid level, lipid, and microbes in the liquid phase (5)

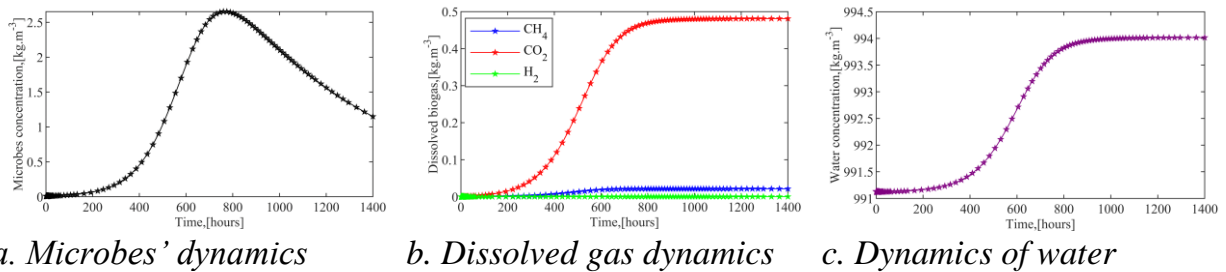


Figure 6.32. Concentration dynamics for microbes, biogas formation and water (5)

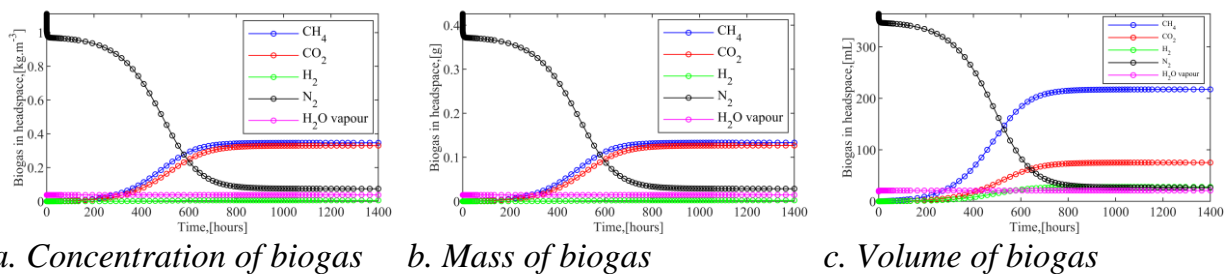
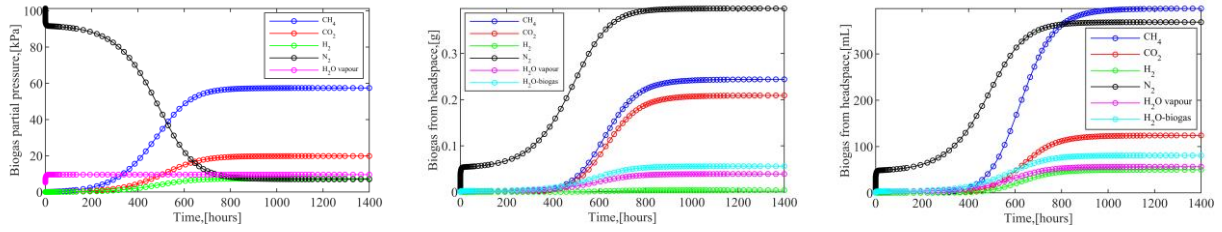
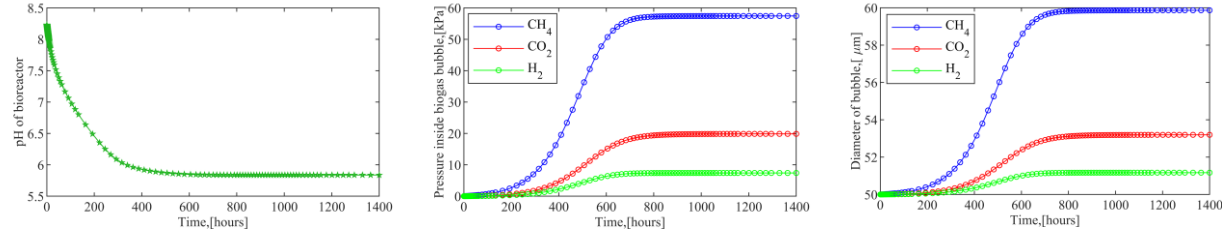


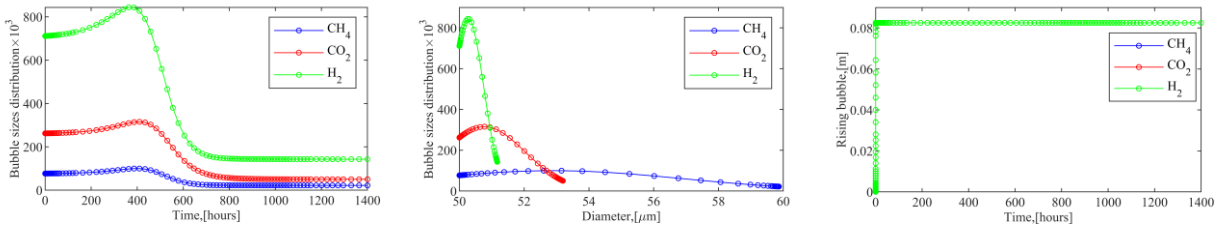
Figure 6.33. Concentration, mass, and volume of biogas obtainable in headspace (5)



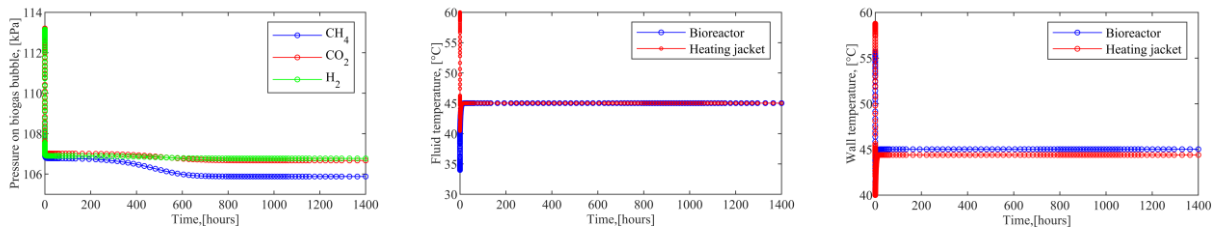
a. Headspace pressure b. Mass of biogas c. Volume of biogas
Figure 6.32. Pressure in headspace, mass, and volume of biogas from headspace (5)



a. pH of bioreactor b. Pressure in bubbles c. Diameter of bubbles
Figure 6.35. pH bioreactor, pressure in bubbles, and diameter of biogas bubbles (5)



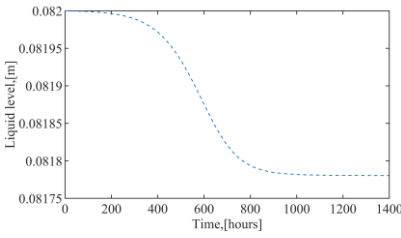
a. Distribution-time b. Distribution-diameter c. Height of bubbles
Figure 6.36. Biogas bubbles distribution and its rising height in liquid phase (5)



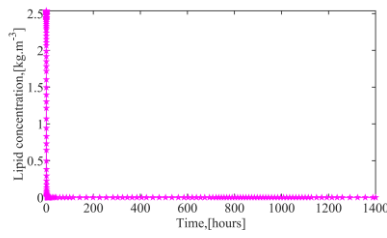
a. Pressure on bubbles b. Fluid temperatures c. Wall temperatures
Figure 6.37. Bubbles surface pressure, fluid, and wall temperature of reaction system (5)

Case-Study-B(T)

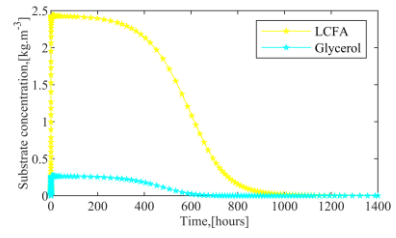
This case study focuses on applying overpressure to investigate the effect of temperature (45 °C) on a complete-batch system.



a. Level dynamics

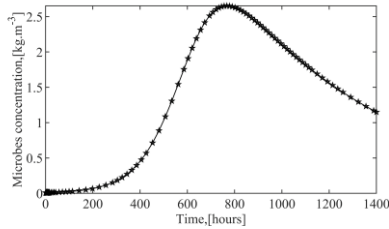


b. Lipid dynamics

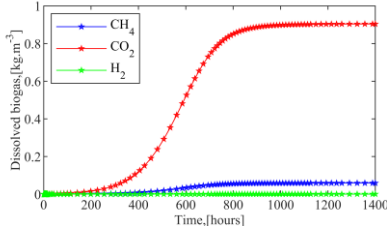


c. Substrate dynamics

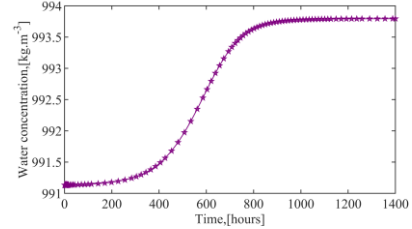
Figure 6.38. Changes in liquid level, lipid, and microbes in the liquid phase (6)



a. Microbes' dynamics

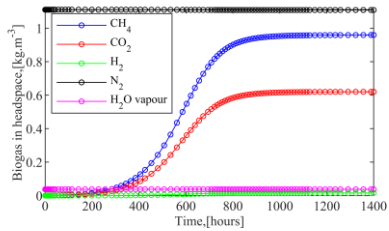


b. Dissolved gas dynamics

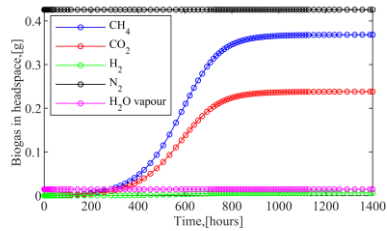


c. Dynamics of water

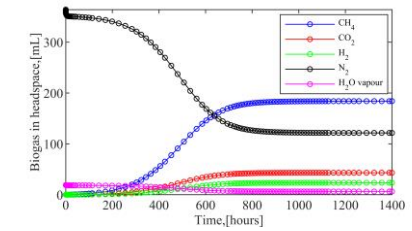
Figure 6.39. Concentration dynamics for microbes, biogas formation and water (6)



a. Concentration of biogas

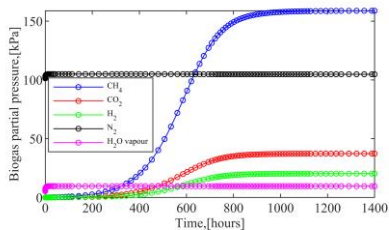


b. Mass of biogas

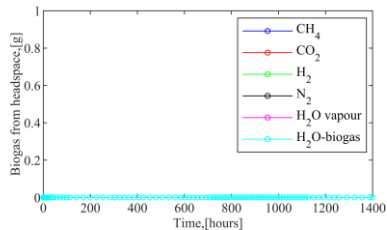


c. Volume of biogas

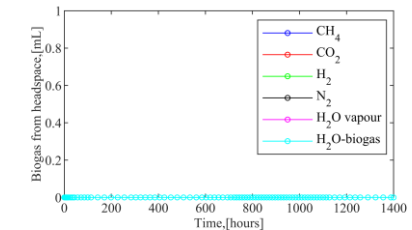
Figure 6.40. Concentration, mass, and volume of biogas obtainable in headspace (6)



a. Headspace pressure

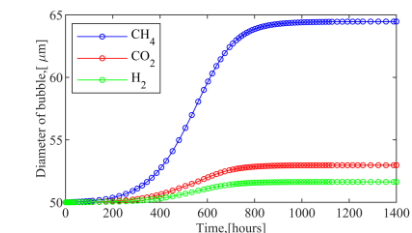
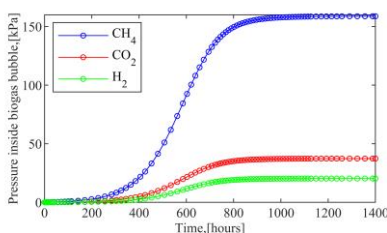
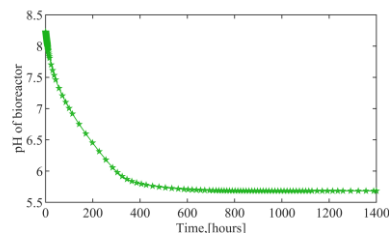


b. Mass of biogas

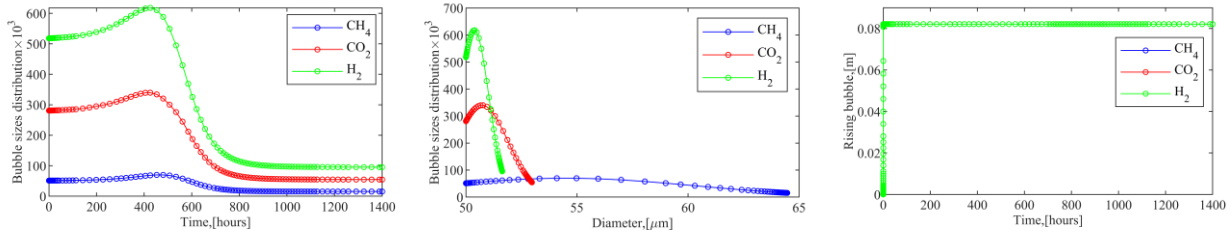


c. Volume of biogas

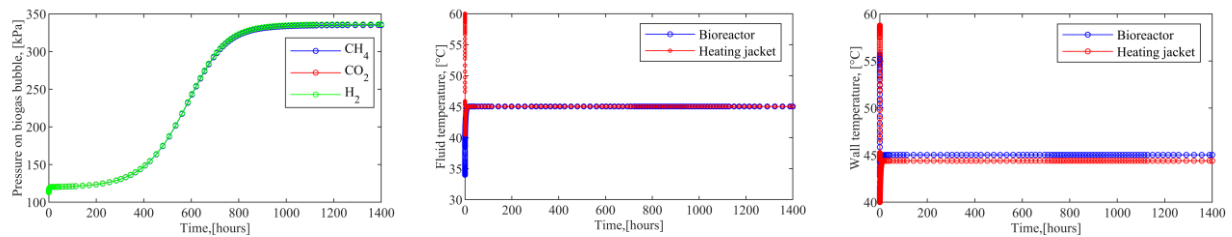
Figure 6.41. Pressure in headspace, mass, and volume of biogas from headspace (6)



a. pH of bioreactor b. Pressure in bubbles c. Diameter of bubbles
Figure 6.42. pH bioreactor, pressure in bubbles, and diameter of biogas bubbles (6)



a. Distribution-time b. Distribution-diameter c. Height of bubbles
Figure 6.43. Biogas bubbles distribution and its rising height in liquid phase (6)

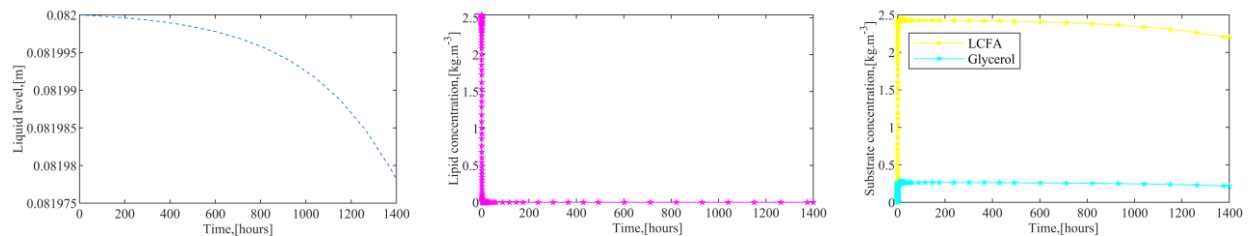


a. Pressure on bubbles b. Fluid temperatures c. Wall temperatures
Figure 6.44. Bubbles surface pressure, fluid, and wall temperature of reaction system (6)

In summary, increasing the temperature of the AD enhances the reaction rate. This favours the production of all biogas species, with a rapid increase in bubble growth, as such a more reduced bubble size distribution.

Case-study-C(T)

Figure (8.45) – (8.51) is an illustration of the AD at ~ 59 °C by setting the heating water flowrate, $q_{hw} = 0.00000050 \text{ m}^3 \cdot \text{s}^{-1}$. It can be observed in all the results, especially Figure (8.46a) that the system has been greatly inhibited.



a. Level dynamics b. Lipid dynamics c. Substrate dynamics
Figure 6.45. Changes in liquid level, lipid, and microbes in the liquid phase (7)

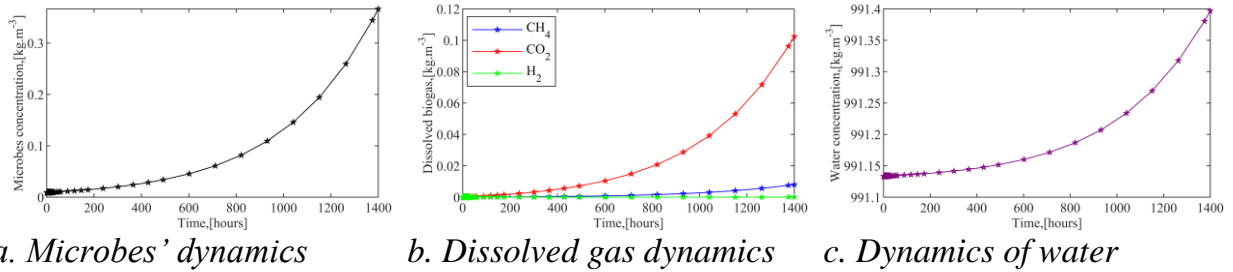


Figure 6.46. Concentration dynamics for microbes, biogas formation and water (7)

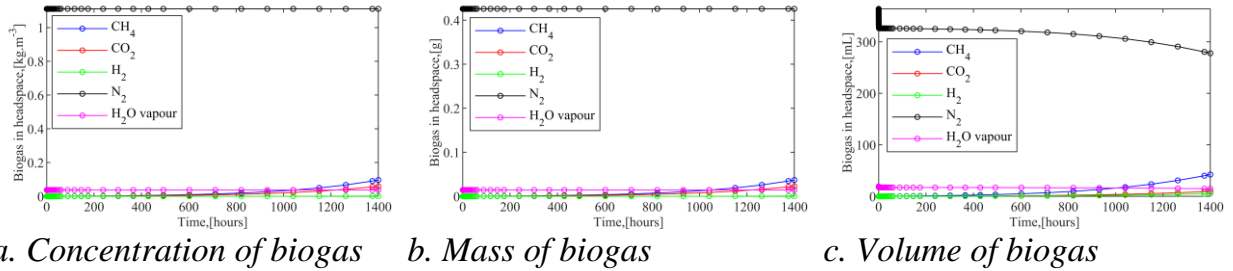


Figure 6.47. Concentration, mass, and volume of biogas obtainable in headspace (7)

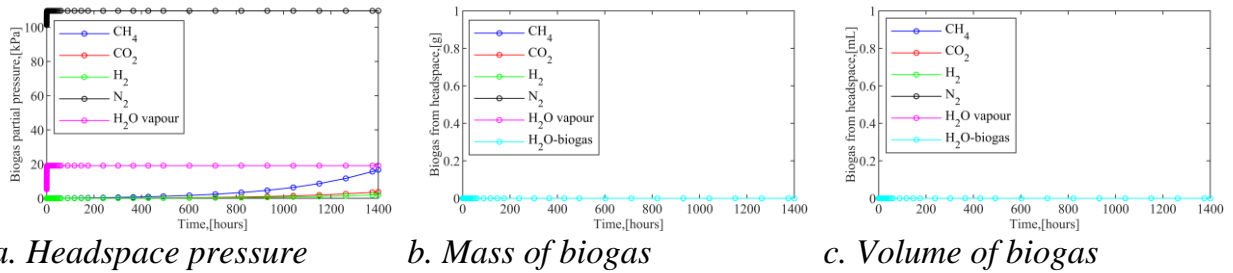


Figure 6.48. Pressure in headspace, mass, and volume of biogas from headspace (7)

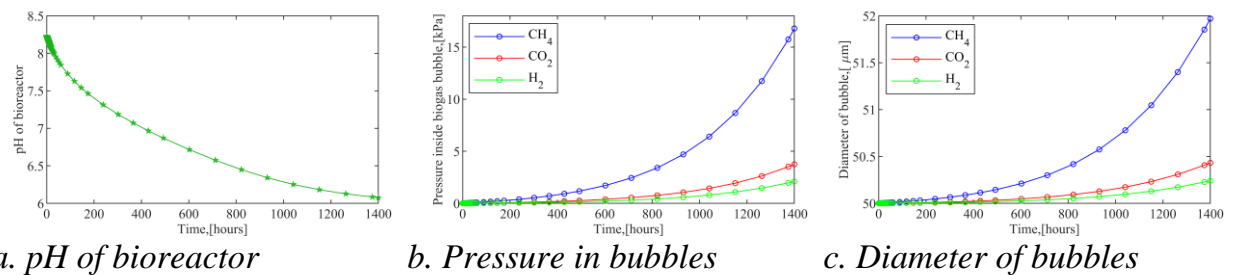
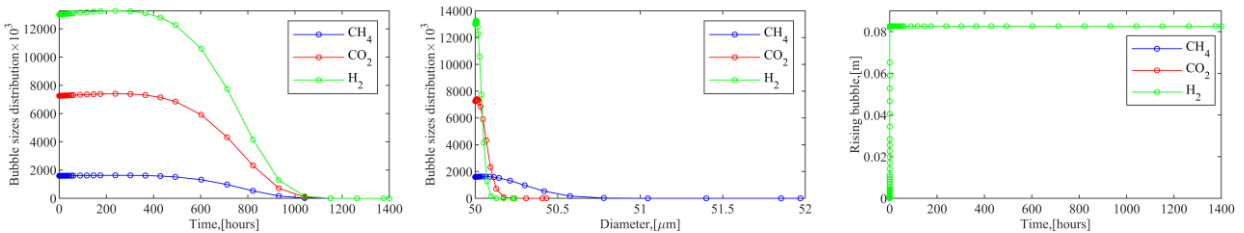
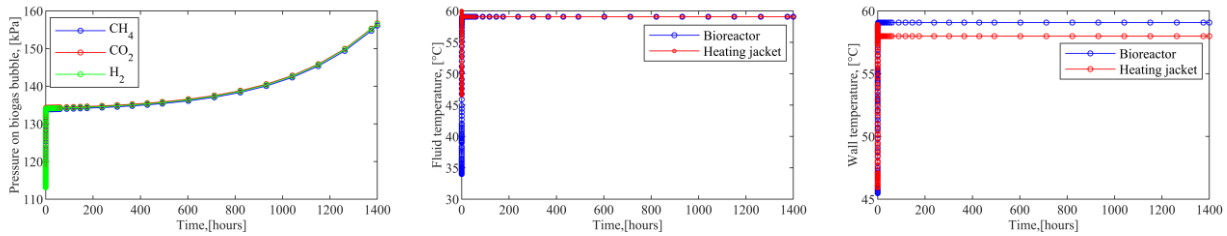


Figure 6.49. pH bioreactor, pressure in bubbles, and diameter of biogas bubbles (7)



a. Distribution-time b. Distribution-diameter c. Height of bubbles
Figure 6.50. Biogas bubbles distribution and its rising height in liquid phase (7)



a. Pressure on bubbles b. Fluid temperatures c. Wall temperatures
Figure 6.51. Bubbles surface pressure, fluid, and wall temperature of reaction system (7)

Table 6.3. Iteratively estimated heat transfer properties for the AD process

Temperature, °C	Heat transfer coefficient, W.m ⁻² . K ⁻¹		Overall heat transfer coefficient, W.m ⁻² . K ⁻¹
	Bioreactor content	Heating water	Bioreactor outer surface
35	1457.640	114.3820	98.98090
45	1570.870	117.6940	101.9860
59	1718.060	133.9400	114.7090

7. Conclusion

In conclusion, based on the simulation results in responds to changes in the operating temperature, pressure, and pH. It can be inferred that the developed SSDM is adequate in modelling the AD process, especially regarding the expected theoretical responds according to Henry’s and Ideal gas laws. In addition to the simplified comparison of the simulation result (at atmospheric condition and consideration of pH inhibition) to the experimental result, which was found to be approximately 40 v/v% of the experimentally produced biogas. Furthermore, to adequately validate the developed SSDM, a comprehensive comparison or optimisation of the model to experimental data on real-time dynamics (i.e., dynamics of substrate, microbes, dissolved and evolved biogas species concentrations, as well as water vapour together with biogas water content) is necessary. Performing such comprehensive model optimisation to fit experimental results would require specialised analytical equipment, as well as a careful development of methodologies. Which are currently beyond the time, and financial limit of this thesis.

7.1. Contribution to science and practice

As a contribution to science, a new simplified AD model based on SSDM has been developed. This model can serve as an alternative to the popular standard Anaerobic digestion model no.1 (**ADM1**), as it can also estimate biogas evolution, as such its headspace pressure. Furthermore, unlike the ADM1 or other multi-step dynamic models. The SSDM developed in this work incorporated a novel model to predict the water evaporation rate from the liquid phase in a closed or partially closed vessel. The model can also be applied to other liquid systems apart from water. Also, the model can predict inherent water content in biogas based on the thermodynamics of water-hydrocarbon phase equilibrium. The pH dynamic in this model has been developed, such that the control of pH via this model is simplified. In addition, the hydrolysis dynamic of the feedstock (i.e., lipid) has been developed to elucidate the effect of temperature. Furthermore, most fluid properties have been modelled as a function of temperature, in addition to modelling the temperature dynamics of the AD, unlike other reported AD models. Therefore, this developed SSDM is most likely the outperform other AD models in evaluating the effect of temperature.

Finally, as a contribution to practice, the SSDM developed in this work can be effectively applied in simulating, optimisation, and control of industrial AD plants. Therefore, it could be applied in the design and sizing, as well as cost estimation of anaerobic bioreactors (as such the AD plant economics) for laboratory-scaled, medium to large-scale industrial biogas plants.

Bibliography

- [1] Demirbaş A, Şahin-Demirbaş A, Hilal Demirbaş A. Global Energy Sources, Energy Usage, and Future Developments. *Energy Sources* 2010;26:191–204. <https://doi.org/10.1080/00908310490256518>.
- [2] Dincer I, Aydin MI. New paradigms in sustainable energy systems with hydrogen. *Energy Convers Manag* 2023;283:116950. <https://doi.org/10.1016/J.ENCONMAN.2023.116950>.
- [3] Borowski PF. Mitigating Climate Change and the Development of Green Energy versus a Return to Fossil Fuels Due to the Energy Crisis in 2022. *Energies (Basel)* 2022;15:9289. <https://doi.org/10.3390/EN15249289>.
- [4] Kumar S, Smith SR, Fowler G, Velis C, Kumar SJ, Arya S, et al. Challenges and opportunities associated with waste management in India. *R Soc Open Sci* 2017;4. <https://doi.org/10.1098/RSOS.160764>.
- [5] Atchike DW, Irfan M, Ahmad M, Rehman MA. Waste-to-Renewable Energy Transition: Biogas Generation for Sustainable Development. *Front Environ Sci* 2022;10:840588. <https://doi.org/10.3389/FENV.S.2022.840588>.
- [6] Yang M, Chen L, Wang J, Msigwa G, Osman AI, Fawzy S, et al. Circular economy strategies for combating climate change and other environmental issues. *Environmental Chemistry Letters* 2022 21:1 2022;21:55–80. <https://doi.org/10.1007/S10311-022-01499-6>.
- [7] Gielen D, Boshell F, Saygin D, Bazilian MD, Wagner N, Gorini R. The role of renewable energy in the global energy transformation. *Energy Strategy Reviews* 2019;24:38–50. <https://doi.org/10.1016/J.ESR.2019.01.006>.
- [8] Ng'andwe P, Ratnasingam J, Mwitwa J, Tembo JC. Wood and Wood Products, Markets and Trade. *Forest Policy, Economics, and Markets in Zambia* 2015:27–66. <https://doi.org/10.1016/B978-0-12-804090-4.00002-1>.
- [9] Tambone F, Scaglia B, D'Imporzano G, Schievano A, Orzi V, Salati S, et al. Assessing amendment and fertilizing properties of digestates from anaerobic digestion through a comparative study with digested sludge and compost. *Chemosphere* 2010;81:577–83. <https://doi.org/10.1016/J.CHEMOSPHERE.2010.08.034>.
- [10] Materazzi M, Foscolo PU. The role of waste and renewable gas to decarbonize the energy sector. *Substitute Natural Gas from Waste: Technical*

- Assessment and Industrial Applications of Biochemical and Thermochemical Processes 2019:1–19. <https://doi.org/10.1016/B978-0-12-815554-7.00001-5>.
- [11] Bušić A, Kundas S, Morzak G, Belskaya H, Mardetko N, Šantek MI, et al. Recent Trends in Biodiesel and Biogas Production. *Food Technol Biotechnol* 2018;56:152–73. <https://doi.org/10.17113/FTB.56.02.18.5547>.
- [12] Varbanov PS, Wang Q, Zeng M, Seferlis P, Ma T, Klemeš JJ, et al. Cooking Oil and Fat Waste Management: A Review of the Current State. *Chem Eng Trans* 2020;81:763–8. <https://doi.org/10.3303/CET2081128>.
- [13] Lobo MG, Dorta E. Utilization and Management of Horticultural Waste. *Postharvest Technology of Perishable Horticultural Commodities* 2019:639–66. <https://doi.org/10.1016/B978-0-12-813276-0.00019-5>.
- [14] Van Hulle SWH, Vesvikar M, Poutiainen H, Nopens I. Importance of scale and hydrodynamics for modeling anaerobic digester performance. *Chemical Engineering Journal* 2014;255:71–7. <https://doi.org/10.1016/J.CEJ.2014.06.041>.
- [15] Jain S, Lala AK, Bhatia SK, Kudchadker AP. Modelling of hydrolysis controlled anaerobic digestion. *Journal of Chemical Technology & Biotechnology* 1992;53:337–44. <https://doi.org/10.1002/JCTB.280530404>.
- [16] Ma J, Frear C, Wang ZW, Yu L, Zhao Q, Li X, et al. A simple methodology for rate-limiting step determination for anaerobic digestion of complex substrates and effect of microbial community ratio. *Bioresour Technol* 2013;134:391–5. <https://doi.org/10.1016/J.BIORTECH.2013.02.014>.
- [17] Batstone DJ, Keller J, Angelidaki I, Kalyuzhnyi S V., Pavlostathis SG, Rozzi A, et al. The IWA Anaerobic Digestion Model No 1 (ADM1). *Water Science and Technology* 2002;45:65–73. <https://doi.org/10.2166/WST.2002.0292>.
- [18] Jiunn-Jyi L, Yu-You L, Noike T. Influences of pH and moisture content on the methane production in high-solids sludge digestion. *Water Res* 1997;31:1518–24. [https://doi.org/10.1016/S0043-1354\(96\)00413-7](https://doi.org/10.1016/S0043-1354(96)00413-7).
- [19] Nielfa A, Cano R, Fdz-Polanco M. Theoretical methane production generated by the co-digestion of organic fraction municipal solid waste and biological sludge. *Biotechnology Reports* 2015;5:14–21. <https://doi.org/10.1016/J.BTRE.2014.10.005>.

- [20] Hill DT, Barth CL. A Dynamic Model for Simulation of Animal Waste Digestion. *Water Pollution Control Federation* 1977;49:2129–43.
- [21] Havlík I, Votruba J, Sobotka M. Mathematical modelling of the anaerobic digestion process: Application of dynamic mass-energy balance. *Folia Microbiol (Praha)* 1986;31:56–68. <https://doi.org/10.1007/BF02928680>.
- [22] Emebu S, Pecha J, Janáčková D. Review on anaerobic digestion models: Model classification & elaboration of process phenomena. *Renewable and Sustainable Energy Reviews* 2022;160:112288. <https://doi.org/10.1016/J.RSER.2022.112288>.
- [23] Fedailaine M, Moussi K, Khitous M, Abada S, Saber M, Tirichine N. Modeling of the Anaerobic Digestion of Organic Waste for Biogas Production. *Procedia Comput Sci* 2015;52:730–7. <https://doi.org/10.1016/J.PROCS.2015.05.086>.
- [24] Šánek L, Pecha J, Kolomazník K. Simultaneous determination of main reaction components in the reaction mixture during biodiesel production. *J Sep Sci* 2013;36:1029–36. <https://doi.org/10.1002/JSSC.201200967>.
- [25] Gao J, Li J, Wachemo AC, Yuan H, Zuo X, Li X. Mass conversion pathway during anaerobic digestion of wheat straw. *RSC Adv* 2020;10:27720–7. <https://doi.org/10.1039/D0RA02441D>.
- [26] Van Der Tempel L, Melis GP, Brandsma TC. Thermal conductivity of a glass: I. Measurement by the glass-metal contact. *Glass Physics and Chemistry* 2000;26:606–11. <https://doi.org/10.1023/A:1007164501169>.

Appendix

A.1. Properties of fluids

The following data were curve-fitted in relation to temperature (K) to model the fluid properties (density, (kg.m⁻³), viscosity (Pa.s), thermal conductivity (W.m⁻¹.k⁻¹), specific heat capacity (J.Kg⁻¹.K⁻¹), etc.

A.2. Hydrogen gas

Applicable within temperature limit, 173 – 398 K.

$$\rho_{\text{H}_2} = 0.4287 \exp(-0.01303T) + 0.1378 \exp(-0.002158T) \quad (\text{A.1})$$

$$\eta_{\text{H}_2} = -1.26 * 10^{-11}T^2 + 2.81 * 10^{-8}T + 1.664 * 10^{-6} \quad (\text{A.2})$$

$$h_{\text{H}_2} = -3.263 * 10^{-7}T^2 + 7.021 * 10^{-4}T + 0.004938 \quad (\text{A.3})$$

$$C_{\text{P-H}_2} = 1.501 * 10^4 \exp(-7.033 * 10^{-5}T) - 1.341 * 10^4 \exp(-0.01183T) \quad (\text{A.4})$$

A.3.Methane gas

Applicable within temperature limit, 180 – 500 K.

$$\rho_{\text{CH}_4} = 3.332 \exp(-0.01194T) + 0.9734 \exp(-0.001899T) \quad (\text{A.5})$$

$$\eta_{\text{CH}_4} = -1.994 * 10^{-11}T^2 + 4.505 * 10^{-8}T - 5.255 * 10^{-7} \quad (\text{A.6})$$

$$h_{\text{CH}_4} = 1.772 * 10^{-7}T^2 + 2.812 * 10^{-5}T + 0.01001 \quad (\text{A.7})$$

$$C_{\text{P-CH}_4} = 2185 \exp(-0.0115T) + 1408 \exp(0.001442T) \quad (\text{A.8})$$

A.4.Carbon dioxide gas

Applicable within temperature limit, 253 – 393 K.

$$\rho_{\text{CO}_2} = 1.744 * 10^{-5}T^2 - 0.01667T + 5.23 \quad (\text{A.9})$$

$$\eta_{\text{CO}_2} = 9.959 * 10^{-6} \exp(0.001867T) - 1.625 * 10^{-5} \exp(-0.00636T) \quad (\text{A.10})$$

$$h_{\text{CO}_2} = 8.183 * 10^{-5}T - 0.007682 \quad (\text{A.11})$$

$$C_{\text{P-CO}_2} = 0.9223T + 575.7 \quad (\text{A.12})$$

A.5.Nitrogen gas

Applicable within temperature limit, 100 – 1300 K.

$$\rho_{\text{N}_2} = 363.9T^{-1.013} \quad (\text{A.13})$$

$$\eta_{\text{N}_2} = 1.208 * 10^{-14}T^3 - 3.997 * 10^{-11}T^2 + 6.688 * 10^{-8}T + 8.824 * 10^{-7} \quad (\text{A.14})$$

$$h_{\text{N}_2} = 2.286 * 10^{-11}T^3 - 6.021 * 10^{-8}T^2 + 1.022 * 10^{-4}T - 2.104 * 10^{-5} \quad (\text{A.15})$$

$$C_{\text{P-N}_2} = 1248 \exp\left(-\left(\frac{T-1734}{2842}\right)^2\right) + 31.72 \exp\left(-\left(\frac{T-285}{294.8}\right)^2\right) + 3198 \exp\left(-\left(\frac{T+373.1}{240.4}\right)^2\right) + 85.96 \exp\left(-\left(\frac{T-97.31}{236.8}\right)^2\right) \quad (\text{A.16})$$

A.6.Ammonia gas

Applicable within temperature limit, 220 – 390 K.

$$\rho_{\text{NH}_3} = 3.303 * 10^{-23}T^{9.426} \quad (\text{A.17})$$

$$\eta_{\text{NH}_3} = 1.682 * 10^{-12}T^3 - 1.395 * 10^{-9}T^2 + 4.201 * 10^{-7}T - 3.453 * 10^{-5} \quad (\text{A.18})$$

$$\begin{aligned} k_{\text{NH}_3} = & 0.08199 \exp\left(-\left(\frac{T-435}{61.33}\right)^2\right) - 2.756 * 10^{-4} \exp\left(-\left(\frac{T-253.8}{35.64}\right)^2\right) \\ & + 0.004923 \exp\left(-\left(\frac{T-351.8}{38.45}\right)^2\right) + 0.03056 \exp\left(-\left(\frac{T-374.4}{190.8}\right)^2\right) \end{aligned} \quad (\text{A.19})$$

$$\begin{aligned} C_{\text{P-NH}_3} = & 3.095 * 10^6 \exp\left(-\left(\frac{T-706.6}{128.4}\right)^2\right) + 6.489 * 10^{13} \exp\left(-\left(\frac{T-707}{64.95}\right)^2\right) \\ & + 1913 \exp\left(-\left(\frac{T-377.2}{102.9}\right)^2\right) + 1997 \exp\left(-\left(\frac{T-437.7}{941}\right)^2\right) \end{aligned} \quad (\text{A.20})$$

A.7.Air

Applicable within temperature limit, 253 – 398 K. Note that density, ρ_{Air} (kg.m^{-3}), Equation (A.21), was estimated using the ideal gas law.

$$\rho_{\text{Air}} = \frac{M_{\text{Air}} P_{\text{atm}}}{RT} \quad (\text{A.21})$$

$$\eta_{\text{Air}} = 2.214 * 10^{-7} T^{0.7757} \quad (\text{A.22})$$

$$k_{\text{Air}} = 0.0002199 T^{0.8373} \quad (\text{A.23})$$

$$C_{\text{P-Air}} = 0.0004002 T^2 - 0.2015 T + 1031 \quad (\text{A.24})$$

A.8.Lipid (Palm oil)

These models are applicable within temperature limit, 293 – 573 K.

$$\rho_{\text{lip}} = -249.4 T^{0.2023} + 1677 \quad (\text{A.25})$$

$$\eta_{\text{lip}} = 8.971 * 10^7 \exp(-0.07078 T) + 0.5186 \exp(-0.01158 T) \quad (\text{A.26})$$

$$k_{\text{lip}} = 122.4 T^{-1.478} + 0.146 \quad (\text{A.27})$$

$$C_{\text{lip}} = 0.003468 T^2 + 0.601 T + 1374 \quad (\text{A.28})$$

A.9.Liquid water

Applicable within temperature limit, 273 – 373 K.

$$\rho_{\text{W}} = -0.003547 T^2 + 1.863 T + 756.4 \quad (\text{A.29})$$

$$\eta_{\text{W}} = 556.6 \exp(-0.04841 T) + 0.0132 \exp(-0.01043 T) \quad (\text{A.30})$$

$$k_{\text{W}} = -9.518 * 10^{-6} T^2 + 0.007335 T - 0.7331 \quad (\text{A.31})$$

$$C_W = 6.865 * 10^{16} \exp\left(-\left(\frac{T + 1.587e^{+04}}{2920}\right)^2\right) + 1.132 * 10^4 \exp\left(-\left(\frac{T - 391.6}{91.14}\right)^2\right) - 9447 \exp\left(-\left(\frac{T - 388.1}{85.41}\right)^2\right) + 2.239 \exp\left(-\left(\frac{T - 298}{16.85}\right)^2\right) \quad (\text{A.32})$$

A.10. Water vapour

These models are applicable within temperature limit, 175 – 500 K. In addition, the heat of vapourisation, $\Delta H_{w_v}^{\text{Evp}}$ (J.kg⁻¹), was also curved fitted, Equation (A.37) with the limit of 275 – 473 K.

$$\rho_{w_v} = \frac{M_W P_{\text{sat}}}{RT} \quad (\text{A.33})$$

$$\eta_{w_v} = 1.12 * 10^{-5} \left(\frac{T}{350}\right)^{1.5} \left(\frac{1414}{T + 1064}\right) \quad (\text{A.34})$$

$$k_{w_v} = 1.952 * 10^{-5} T^{1.258} + 0.01811 \quad (\text{A.35})$$

$$C_{w_v} = 0.001009T^2 - 0.3576T + 1881 \quad (\text{A.36})$$

$$\Delta H_{w_v}^{\text{Evp}} = -3.42T^2 - 200.9T + 2.806 * 10^6 \quad (\text{A.37})$$

A.11. Properties of solid

Considering that the laboratory scale bioreactor is made of glass, the thermal conductivity of glass, Equation (A.38), as reported in literature [26] was applied.

$$k_{w_v} = -5.268T^{-0.78} + 1.244 \quad (\text{A.38})$$

A.12. Fluid mixing rule

In simulating the interaction of fluids to estimate the average properties (p) of type (i) of mixed gaseous and liquid phase with different species (i) were estimated based on the linear mixing rule, Equation (A.39). Where x is the fraction of specie (j) in the gaseous or liquid phase being considered with J total number of species in the various phases.

$$p_i = \sum_j^J x_j p_i \quad (\text{A.39})$$

A.13.Auxiliary equations

The mass and volumetric outflow from the gaseous outlet of the bioreactor can be deduced from the integration of Equation (A.41) – (A.42). While the remaining amount in the bioreactor is given by Equation (A.43) – (A.44).

$$\dot{m}_{o-G_{j^*}} = \frac{dm_{o-G_{j^*}}}{dt} = q_{o-G} G_{j^*} \quad (\text{A.41})$$

$$\dot{V}_{o-G_{j^*}} = \frac{dV_{o-G_{j^*}}}{dt} = \frac{\dot{m}_{o-G_{j^*}} RT}{P_G M_{j^*}} \quad (\text{A.42})$$

$$m_{G_{j^*}} = V_G G_{j^*} \quad (\text{A.43})$$

$$V_{G_{j^*}} = \frac{m_{G_{j^*}} RT}{P_G M_{j^*}} \quad (\text{A.44})$$

List of figures

Figure 2.1. Illustrative scheme of anaerobic digestion stages [22]	5
Figure 3.1. Illustration of degradation level considered in the multi-step dynamic models	7
Figure 4.1. Description of anaerobic digestion in a continuous stirred tank reactor (CSTR) type bioreactor with material and heat transfer.....	9
Figure 5.1. Experimental setup utilised for the anaerobic digestion	16
Figure 6.1. Illustration of hydrolysis kinetic, and Gaussian model for lipid degradation.....	19
Figure 6.2. Biogas production, and maximum microbe specific growth rate	20
Figure 6.3. Changes in liquid level, lipid, and microbes in the liquid phase (1).....	21
Figure 6.4. Concentration dynamics for microbes, biogas formation and water (1).....	21
Figure 6.5. Concentration, mass, and volume of biogas obtainable in headspace (1)	21
Figure 6.6. Pressure in headspace, mass, and volume of biogas from headspace (1).....	21
Figure 6.7. pH bioreactor, pressure in bubbles, and diameter of biogas bubbles (1).....	21
Figure 6.8. Biogas bubbles distribution and its rising height in liquid phase (1).....	22
Figure 6.9. Bubbles surface pressure, fluid, and wall temperature of reaction system (1)	22
Figure 6.10. Changes in liquid level, lipid, and microbes in the liquid phase (2).....	22
Figure 6.11. Concentration dynamics for microbes, biogas formation and water (2).....	23
Figure 6.12. Concentration, mass, and volume of biogas obtainable in headspace (2).....	23
Figure 6.13. Pressure in headspace, mass, and volume of biogas from headspace (2).....	23
Figure 6.14. pH bioreactor, pressure in bubbles, and diameter of biogas bubbles (2).....	23
Figure 6.15. Biogas bubbles distribution and its rising height in liquid phase (2).....	23
Figure 6.16. Bubbles surface pressure, fluid, and wall temperature of reaction system (2)	24

Figure 6.17. Changes in liquid level, lipid, and microbes in the liquid phase (3).....	24
Figure 6.18. Concentration dynamics for microbes, biogas formation and water (3).....	24
Figure 6.19. Concentration, mass, and volume of biogas obtainable in headspace (3).....	25
Figure 6.20. Pressure in headspace, mass, and volume of biogas from headspace (3)	25
Figure 6.21. pH bioreactor, pressure in bubbles, and diameter of biogas bubbles (3)	25
Figure 6.22. Biogas bubbles distribution and its rising height in liquid phase (3).....	25
Figure 6.23. Bubbles surface pressure, fluid, and wall temperature of reaction system (3)	25
Figure 6.24. Changes in liquid level, lipid, and microbes in the liquid phase (4).....	26
Figure 6.25. Concentration dynamics for microbes, biogas formation and water (4).....	26
Figure 6.26. Concentration, mass, and volume of biogas obtainable in headspace (4).....	26
Figure 6.27. Pressure in headspace, mass, and volume of biogas from headspace (4)	27
Figure 6.28. pH bioreactor, pressure in bubbles, and diameter of biogas bubbles (4)	27
Figure 6.29. Biogas bubbles distribution and its rising height in liquid phase (4).....	27
Figure 6.30. Bubbles surface pressure, fluid, and wall temperature of reaction system (4)	27
Figure 6.31. Changes in liquid level, lipid, and microbes in the liquid phase (5).....	28
Figure 6.32. Concentration dynamics for microbes, biogas formation and water (5).....	28
Figure 6.33. Concentration, mass, and volume of biogas obtainable in headspace (5).....	28
Figure 6.32. Pressure in headspace, mass, and volume of biogas from headspace (5)	29
Figure 6.35. pH bioreactor, pressure in bubbles, and diameter of biogas bubbles (5)	29
Figure 6.36. Biogas bubbles distribution and its rising height in liquid phase (5).....	29
Figure 6.37. Bubbles surface pressure, fluid, and wall temperature of reaction system (5)	29
Figure 6.38. Changes in liquid level, lipid, and microbes in the liquid phase (6).....	30
Figure 6.39. Concentration dynamics for microbes, biogas formation and water (6).....	30
Figure 6.40. Concentration, mass, and volume of biogas obtainable in headspace (6).....	30
Figure 6.41. Pressure in headspace, mass, and volume of biogas from headspace (6)	30
Figure 6.42. pH bioreactor, pressure in bubbles, and diameter of biogas bubbles (6)	31
Figure 6.43. Biogas bubbles distribution and its rising height in liquid phase (6).....	31
Figure 6.44. Bubbles surface pressure, fluid, and wall temperature of reaction system (6)	31
Figure 6.45. Changes in liquid level, lipid, and microbes in the liquid phase (7).....	31
Figure 6.46. Concentration dynamics for microbes, biogas formation and water (7).....	32
Figure 6.47. Concentration, mass, and volume of biogas obtainable in headspace (7).....	32
Figure 6.48. Pressure in headspace, mass, and volume of biogas from headspace (7)	32
Figure 6.49. pH bioreactor, pressure in bubbles, and diameter of biogas bubbles (7)	32
Figure 6.50. Biogas bubbles distribution and its rising height in liquid phase (7).....	33
Figure 6.51. Bubbles surface pressure, fluid, and wall temperature of reaction system (7)	33

List of tables

Table 3.1. Theoretical yield estimate of the substrate from feedstock, biogas and microbes from the substrate, ammonia from microbes for lipid (triglyceride with oleic acid).....	8
Table 5.1. Average physicochemical properties, and composition of sludge sample	15
Table 5.2. Simulation parameters based on laboratory scale, and literature review	17
Table 6.1. Hydrolysis model based on the single-step curve-fitting methods.....	19
Table 6.2. Ratkowsky constants for estimation of maximum specific growth rate.....	20
Table 6.3. Iteratively estimated heat transfer properties for the AD process	33

List of Abbreviations

Abbreviation	Definition
AD	Anaerobic digestion
ADM1	Anaerobic Digestion Model No. 1
AM2	Acidogenesis-methanogenesis-two-steps
ATP	Adenosine triphosphate
BMP	Biochemical Methane Potential
BOD	Biochemical oxygen demand
CFRT	Closed floating roof tank
CSTR	Continuous Stirred Tank Reactor
CNG	Compressed natural gas
COD	Chemical oxygen demand
DAGs	Diacylglycerols
EFRT	External floating roof tank
FA	Fatty acids
FFA	Free fatty acids
FRT	Fixed roof tank
FTIR	Fourier-transform infrared spectroscopy
HRT	Hydraulic retention time
HW	Heating or hot water
HJ	Heating jacket
IFRT	Internal floating roof tank
LC	Level controller
LCFA	Long-chain fatty acid
LNG	Liquefied natural gas
MAGs	Monoacylglycerols
MSDM	Multi-step-degradation model
OLR	Organic loading rate
PC	Pressure controller
pHC	pH controller
SRT	Solids retention time
SSDM	Single-step-degradation model
TAGs	Triacylglycerols
TC	Temperature controller
TKN	Total kjeldahl nitrogen
TOC	Total organic carbon
TS	Total solid
TSS	Total suspended solids

VS	Volatile solid
VSS	Volatile suspended solids

List of symbols

Symbols (unit)	Definition
a ($\text{mg}\cdot\text{g}^{-1}\cdot\text{s}^{-1}$); a (s^{-1})	Biogas production constant; Rate constants
a^* ($\text{mg}\cdot\text{g}^{-1}\cdot\text{time}^{-1}$)	Biogas production constant
a_j (m^{-1})	Specific interfacial area of gas per unit volume of liquid
A (m^2); A ($\text{mg}\cdot\text{g}^{-1}$)	Area of bioreactor; Biogas production potential
A_a (s^{-1})	Preexponential factor
A_H (m^2)	Area of heating jacket
b ($\text{mg}\cdot\text{g}^{-1}\cdot\text{s}^{-2}$); b (s^{-1})	Biogas production constant; Rate constants
b^* (s^{-1})	Biogas production time constant
b_{ij}	Coefficients of interfacial tension polynomial model
B_j ($\text{kg}\cdot\text{m}^{-3}$)	Microbes' concentration
c (s^{-1})	Biogas production time or rate constant
C_p ($\text{J}\cdot\text{kg}^{-1}\cdot\text{K}^{-1}$)	Specific heat capacity
d_j (m)	Biogas bubble diameter
$d_{j,h}$ (m)	Gas bubble diameters at specific height in the liquid
$d_{j,m}$ (m)	Mean diameter of the gas bubble
$d_{j,m\log}$ (m)	Natural logarithm of mean of bubble diameter
d_{S_j} (m)	Sauter mean diameter
d_{st} (m)	Diameter of impeller
D_R (m)	Bioreactor diameter
D_H (m)	Heating jacket hydraulic inner diameter
D_L ($\text{m}^2\cdot\text{s}^{-1}$)	Diffusivity of biogas species in liquid
\bar{D}_R (m)	Logarithmic mean diameter of bioreactor
\bar{D}_H (m)	Logarithmic mean hydraulic diameter of heating jacket
$e = \exp(1)$	Exponential constant
E_a ($\text{J}\cdot\text{mol}^{-1}$)	Activation energy
$f(x)$	Biogas yield
F ($\text{kg}\cdot\text{m}^{-3}$)	Feedstock/macronutrients concentration
G ($\text{kg}\cdot\text{m}^{-3}$)	General or headspace biogas concentration
G_D ($\text{kg}\cdot\text{m}^{-3}$)	Liquid biogas concentration
G_s ($\text{m}^{-3}\cdot\text{kg}^{-1}$)	Gas production factor
Gr	Grashof number
h_j (m)	Height of the biogas bubble specie in the liquid phase
h_L (m)	Level of the liquid in bioreactor
h_R (m)	Total height of bioreactor
k (s^{-1})	Rate constants
$K_{aj\pm}$ (kgmole)	Disassociation constant
K_d (s^{-1})	Microbe death rate
k_{hyd} (s^{-1})	Rate constants
K_H ($\text{kg}\cdot\text{m}^{-3}\cdot\text{Pa}^{-1}$)	Henry's constant
K_{lipid} (s^{-1})	Hydrolysis rate constant
K_La (s^{-1})	Mass transfer coefficient
K_{mB} (time^{-1})	Maintenance coefficient

$k_T(K^{-1})$	Temperature constant
$k_p(Pa.m^3.s^{-1})$	Pipe resistance coefficient
$k_0(hr^{-1})$	Preexponential factor of the reaction
$L_c(m)$	Characteristic length
$\dot{m}(kg.s^{-1})$	Mass flowrate
$M(kg.kgmole^{-1})$	Molecular mass
n	Number of process factors; order sequence of the polynomial model
$n_b(kgmol)$	Biogas compositional term
$\dot{n}(kgmole.s^{-1})$	Molar flowrate
n_K	Factor for mass transfer coefficient
$n_{st}(rps)$	Impeller speed of bioreactor
$N(kgmol)$	Compositional term
N_p	Power number of the stirrer
N_{Re}	Reynold number of stirring of bioreactor
$p(pa)$	Partial pressure of biogas bubble
$P(pa)$	Partial pressure in headspace
$P_G(pa)$	Total pressure of biogas species
pH_{ul} and pH_{ll}	Upper and lower pH limits
$P_{Mix}(W)$	Stirring power
$P_{N_2}(pa)$	Pressure of inert gas or nitrogen
$P_R(pa)$	Fixed or desired operating pressure of the bioreactor
$P_{sw}(pa)$	Saturated vapour pressure
$p_T(pa)$	Total pressure on biogas bubble
Pr	Prandtl number
$q_{c-L}(m^{-3}.s^{-1})$	Controller volumetric flowrate for pH control
$q_{i-L}(m^{-3}.s^{-1})$	Input volumetric flowrate of liquid
$q_{o-G}(m^{-3}.s^{-1})$	Output volumetric flowrate of gaseous and vapour outlet of bioreactor
$q_{o-GG}(m^{-3}.s^{-1})$	Flowrate of biogas or gaseous component only in q_{o-G}
$q_{o-L}(m^{-3}.s^{-1})$	Output volumetric flowrate of liquid
$q_{i-hw} \equiv q_{o-hw} \equiv q_{hw}(m^{-3}.s^{-1})$	Flowrate of heating or hot water
$Q_{HE}(W)$	Heating energy from hot water
$Q_{H-En}(W)$	Heat loss from heating jacket to the environment or surrounding
$Q_{R-En}(W)$	Heat loss to environment from bioreactor
$r_{Ri}(m)$	Radius of the liquid in bioreactor, i.e., inner
$R(pa.kgmol^{-1}.k^{-1})$	Ideal gas constant
$R_{AD}(kg.m^{-3}.s^{-1})$	Rate of anaerobic digestion
$R_{Bd}(kg.m^{-3}.s^{-1})$	Death rate of biomass
$R_{Bg}(kg.m^{-3}.s^{-1})$	Growth rate of biomass
$R_{B/A}(kg.m^{-3}.s^{-1})$	Conversion rate of acetic acid to biomass
$R_{B/S}(kg.m^{-3}.s^{-1})$	Conversion rate of substrate to biomass
$R_{B/\gamma}(kg.m^{-3}.s^{-1})$	Conversion rate of intermediates acid to biomass
$R_e(kg.m^{-3}.s^{-1})$	Evolution of biogas bubble from liquid to gas headspace
$R_E(kg.m^{-3}.s^{-1})$	Evolution of biogas from liquid to gas headspace
$R_{Evap}(kg.s^{-1})$	Rate of evaporation of water
Re	Reynold number due to fluid flow
$R_F(kg.m^{-3}.s^{-1})$	Consumption rate of feedstock
$R_{G/A}(kg.m^{-3}.s^{-1})$	Conversion rate of acetic acid to biogas
$R_{G/\gamma}(kg.m^{-3}.s^{-1})$	Conversion rate of intermediates to biogas
$R_{max}(mg.g^{-1}.s^{-1})$	Maximal biogas production rate
$R_S(kg.m^{-3}.s^{-1})$	Formation rate of substrate

$R_{A/S}$ (kg.m ⁻³ .s ⁻¹)	Conversion rate of substrate to acetic acid
$R_{A/I}$ (kg.m ⁻³ .s ⁻¹)	Consumption rate of intermediates to acetic acid
$R_{I/S}$ (kg.m ⁻³ .s ⁻¹)	Conversion rate of substrate to intermediates
S (kg.m ⁻³)	Substrates concentration
S_0 (kg.m ⁻³)	Initial substrate concentration
Sc	Schmidt number
t (s)	Digestion time
t_0 (s)	Time when the maximal biogas production rate occurs
T (K)	AD temperature
T_C (K)	Critical temperature
T_f (K)	Film temperature
T_{hw} (K)	Temperature heating water
T_H (K)	Heating jacket wall temperature
T_{min} and T_{max} (K)	Minimum and maximum temperature tolerance of microbes
T_O (K)	Reference temperature of hydrolysis reaction
T_{wc} (K)	Cold side wall temperature of bioreactor
T_{wh} (K)	Hot side wall temperature of bioreactor
u (m.s ⁻¹)	Velocity of fluid
u_b (m.s ⁻¹)	Terminal or rising velocity of the bubble
U_{HE} (W.m ⁻² .K ⁻¹)	Overall heat coefficient of bioreactor with heating jacket
U_{H-En} (W.m ⁻² .K ⁻¹)	Overall heat coefficient of heating jacket with environment
v (m ³)	Volume of biogas bubble
V_G (m ³)	Gas headspace volume
V_{hw} (m ³)	Volume of heating jacket or heating water
v_{H_2O} (m ³ .kgmol ⁻¹)	Average molecular volume of water
V_L (m ³)	Liquid volume
V_R (m ³)	Constant control volume
V_t (m ³)	Volume of biogas generated over a time, t
V_∞ (m ³)	Total volume of biogas produced
W_{H_2O} (kg H ₂ O per m ³ gas)	Inherent moisture accompanying biogas output from the bioreactor
w_v	Water vapour concentration
x_i and x_j	Represent the process factors (pH, temperature, etc.)
x_{j^*} and y_{j^*}	Liquid and gaseous fraction of specie, j^* , in liquid and gaseous phase
y (mg.g ⁻¹ . s ⁻¹) ; y	Biogas production rate; Generic output of data
$Y_{B/S}$ (kg.kg ⁻¹)	Microbe yield from substrate
Y_{cat}	Cation yield from microbes
$Y_{GD/S}$ (kg.kg ⁻¹)	Biogas yield from substrate
$Y_{S/F}$ (kg.kg ⁻¹)	Substrate yield from feedstock
\bar{y}	Mean output of data
\hat{y}	Model output
$[Z]$ (kgmoles.m ⁻³)	Ionic molar concentration
ΔH_{AD} (J.kgmoles ⁻¹)	Heat of reaction of the anaerobic reaction
ΔH_{Evap} (J.kg ⁻¹)	Latent heat of vapourisation of water
$\Delta\rho$	Change in density
ΔT (K)	Temperature difference between fluid and wall
$a, b, c, d,$ and e	Elemental stoichiometric ratio of generic substrate
α_j (m ⁻¹)	Specific interfacial area of gas bubble per unit volume of liquid
α (s ⁻¹)	Rate constants
σ, β & δ	Dimensionless shape factors
\mathcal{A} (kg.m ⁻³)	Acetic acid concentration

$\mathcal{B}(\text{K}^{-1})$	Exponential constant
β	Fluid thermal expansion coefficient
β_o	Model constant
β_i	Coefficient for linear term
β_{ii}	Coefficient for quadratic term
β_{ij}	Coefficient for interactive term
$\mathcal{D} (\text{s}^{-1})$	Bioreactor dilution rate
$\dot{h}_{\text{Air}}(\text{W.m}^{-2}.\text{K}^{-1})$	Heat transfer coefficient of air
$\dot{h}_{\text{H}}(\text{W.m}^{-2}.\text{K}^{-1})$	Heat transfer coefficient of fluid in heating jacket
\dot{h}_{L} and \dot{h}_{G} ($\text{W.m}^{-2}.\text{K}^{-1}$)	Represent the liquid and gas portion of \dot{h}_{R}
$\dot{h}_{\text{R}}(\text{W.m}^{-2}.\text{K}^{-1})$	Heat transfer coefficient of fluid in bioreactor
\dot{i}	Inhibition of various biogas species
\mathbb{I}	Inhibitory concentration, e.g., S , \mathcal{P} and pH
$\mathcal{J} (\text{kg.m}^{-3})$	Intermediates concentration
$\mathcal{K}_b (\text{kg.m}^{-3})$	Kinetic parameter
\mathcal{K}_{CH}	Kinetic parameter
$\mathcal{K}_{i-i} (\text{kg.m}^{-3})$	Inhibition parameter
$\mathcal{K}_s (\text{kg.m}^{-3})$	Half-saturation coefficient
\mathcal{K}_1 & $\mathcal{K}_2 (\text{kg.m}^{-3})$	Kinetic parameters
$k(\text{W.m}^{-1}.\text{K}^{-1})$	Thermal conductivity
ζ_*	Standard deviation of the bubble diameter
$\zeta_{*\log}$	Natural logarithm standard deviation of bubble diameter
n	Number of substrate-binding sites per enzyme molecules
n_o	Fitting constant unique to the system
$\eta_{\text{L}}(\text{Pa.s})$	Viscosity of liquid
Θ	Stirrer characteristic constant
Φ_{B}	Fraction of substrate converted to microbe biomass
Φ_{G}	Fraction of substrate converted to biogas
$\Phi_{\text{H}_2\text{O}}$	Fugacity coefficient of water
Φ_{V}	Volatile fraction of the feedstock
$\mathcal{P} (\text{kg.m}^{-3})$	Product concentration
$\rho_{\text{L}}(\text{kg.m}^{-3})$	Density of liquid
$\rho_i (\text{kg.m}^{-3})$	Density of biogas species
$q (\text{m}^3.\text{kmole}^{-1})$	Molar volume
$\tau (\text{N.m})$	Torque of stirrer
$\mu (\text{s}^{-1})$	Specific microbe growth rate
$\mu_{\text{max}}(\text{s}^{-1})$	Maximum microbe growth rate
$\mu_{\text{max,a}}$ and $\mu_{\text{max,m}}(\text{s}^{-1})$	Maximum microbe growth rate for acidogenes and methanogens
ψ^o	Chemical potential
$\omega_{\text{F}_{j_o}}$	Mass fraction of the specific molecule in feedstock
$\delta_{\text{G}}(\text{kg}^{-1})$	Ideal gas conversion factor
$\lambda(\text{s})$	Lag time
χ	Volumetric fraction of biogas produced
x	Thickness of bioreactor or heating jacket
Υ	pH inhibitory constant
$\gamma_{\text{L}_{j_*}}(\text{N.m}^{-1})$	Interfacial tension between the biogas bubble species and liquid
$\gamma(\text{N.m}^{-1})$	Average interfacial tension of the biogas with the liquid phase

List of subscripts

Subscript	Definition
c	Controller (specifically pH controller)
G	Gaseous
Gw	Gaseous water content
H	Heating jacket
i	Input, inner/internal
<i>i</i>	Inhibitory species e.g., S, [H ⁺] and pH
<i>j</i> = 1, 2, ..., n	Indicates the number of species or order being considered
<i>j</i> * = CH ₄ , CO ₂ , H ₂ , etc.	Represents the various biogas species
<i>j</i> _o = Lipid, protein, etc.	Specific molecule in feedstock
L	Liquid
o	Output, outer
R	Bioreactor
w	Water or wall
w _v	Water vapour

List of publications

Journal Articles	
	Samuel Emebu, Raphael Olabanji Ogunleye, Eva Achbergerová, Lenka Vítková, Petr Ponížil, Clara Mendoza Martinez. Review and proposition for model-based multivariable-multiobjective optimisation of extrusion-based bioprinting. Applied Materials Today , Vol. 34, October 2023, 101914
	Samuel Emebu, Clara Mendoza Martinez, Osaze Omoregbe, Aleksii Mankonen, Ebuka A. Ogbuoji, Ibrahim Shaikh, Even Pettersen, Marek Kubalčík, & Charity Okieimen. Design, techno-economic evaluation, and optimisation of renewable methanol plant model: Finland case study. Chemical Engineering Science , Vol. 278, 2023, 118888
	Samuel Emebu, Jiří Pecha, Dagmar Janáčová. Review on anaerobic digestion models: Model classification & elaboration of process. Renewable and Sustainable Energy Reviews , Vol. 160, 2022, 112288.
	Samuel Emebu, Marek Kubalčík, Christoph Josef Backi & Dagmar Janáčová. A comparative study of linear and nonlinear optimal control of a three-tank system. ISA Transactions , Vol. 132, 2023, Pp. 419-427.
	Christoph Josef Backi, Samuel Emebu, Sigurd Skogestad & Brian Arthur Grimes. A simple modeling approach to control emulsion layers in gravity separators. Computer Aided Chemical Engineering , Vol. 46, 2019, Pp. 1159-1164.
	S. Emebu, O. Osaikhuiwuomwan, A. Mankonen, C. Udoye, C. O. Okieimen & D. Janáčová. Influence of moisture content, temperature, and time on free fatty acid in stored crude. Scientific Reports , Vol. 12(1), 2022.
	Alves Elem Patricia Rocha, Orlando Salcedo-Puerto, Jesús Nuncira, Samuel Emebu, & Clara Mendoza-Martinez. Renewable Energy Potential and CO ₂ Performance of Main Biomasses Used in Brazil. Energies , Vol.16(9), 2023, 3959.

	<p>Ogunleye, Raphael Olabanji, Sona Rusnakova, Milan Zaludek, and Samuel Emebu. The Influence of Ply Stacking Sequence on Mechanical Properties of Carbon/Epoxy Composite Laminates. Polymers, Vol. 14(24), 2022, 5566.</p> <p>Oghenekohwiroro Edjere, Justina E. Ukpebor, Samuel Emebu & Felix E. Okieimen. Preliminary studies of Organochlorine Pesticides (OCPs) in sediment, water and fish samples from Ethiope river, Abraka axis, southern Nigeria. International Letters of Natural Sciences, Vol. 80, 2020, pp. 1-12.</p> <p>E. A. Elimian, S. Emebu, C. O. Okieimen, G. O. Madojemu & G. E. Eluro. Optimization of Non-Competitive Adsorption of Benzene, Toluene and Xylene (BTX) from Aqueous Solutions using Activated Orange Peels. Technical Transactions of Materials Science and Technology Society of Nigeria, Vol. 2, 2019, pp 209-214</p>
Conference	<p>Ibrahim Shaikh, Samuel Emebu, Radek Matušů. Robust H_∞ controller design for satellite systems with uncertain inertia matrix: A linear matrix inequality approach. CoMeSySo 2023 conference. 12 – 14th, Online, October 2023</p> <p>Samuel Emebu, Lubomír Šánek, Jakub Husár, Jiří Pecha, & Dagmar Janáčová. Modelling the kinetics of anaerobic hydrolysis of lipid-rich-waste: Elucidation of the effect of temperature. BIORESTEC-2023 conference, Lake Garda Italy, 14–17th, May 2023.</p>
Manuscript	<p>Sohaibullah Zarghoon, Samuel Emebu, Radek Matušů, Cyril Belavý, Lukáš Bartalský, Clara Mendoza Martinez. Modelling, simulation, and control of induction heating of steel billet based on full-state feedback LQR controllers. Manuscript is currently being reviewed by the Journal of Process Control</p> <p>Samuel Emebu, Lubomír Šánek, Jakub Husár, Jiří Pecha, & Dagmar Janáčová. Modelling the kinetics of anaerobic hydrolysis of lipid-rich-waste: Elucidation of the effect of temperature. Manuscript has been submitted to the journal of Materials today sustainability.</p> <p>Samuel Emebu, Clara Mendoza Martinez, Aleksi Mankonen, Raphael Olabanji Ogunleye, Ojeaga Evans Imanah, Marek Kubalčík, Dagmar Janáčová & Felix Ebhodaghe Okieimen. Guide to adequate curve-fitting of models Comparison between multi-step, and single-step curve-fitting techniques. Manuscript has been prepared for submission</p>

Curriculum vitae

Personal information

Name Samuel Emebu
Address Budovatelska, 4810, 760 05, Zlin, Czechia
Telephone +420733458998
Email emebu@utb.cz
Date of birth 19-09-1988
Gender Male
Nationality Nigerian (Nigeria)

Education and training

2020 – 2023 Engineering informatics (Doctoral studies)
Tomas Bata University, Zlin, Czech Republic
2016 – 2018 Chemical Engineering-Process Systems (master's degree Programme)
Norwegian University of Science and Technology, Trondheim, Norway
2007 – 2012 Chemical Engineering (bachelor's degree Programme)
University of Benin, Benin city, Nigeria. Department of Chemical Engineering

Digital skills MATLAB & Simulink, Python for statistic, Overleaf/Latex, Aspen HYSYS, Aspen PLUS, SOLIDWORKS, Microsoft Office.

Project-Grant

2021 – 2023 Hydrolysis of lipid-rich waste within the scope of anaerobic digestion
Funded by the Internal Grant Agency (IGA/CebiaTech/2021/002, IGA/CebiaTech/2022/002, IGA/CebiaTech/2023/004) of Tomas Bata University
2021 – 2023 Development of biopolymer-based hydrogel for micro-extrusion (Modelling and optimisation)
Funded by the Junior Grant Program, through the Ministry of Education, Youth & Sport (Czech Republic) and the European Union

The Mathematical Modelling of Waste Fats Treatment into Biogas

Matematické modelování zpracování odpadních tuků na bioplyn

Doctoral Thesis Summary

Published by: Tomas Bata University in Zlín
nám. T. G. Masaryka 5555, 760 01 Zlín, Czech Republic

Edition: published electronically

Typesetting by: Ing. Samuel Emebu, Ph.D.

This publication has not undergone any proofreading or editorial review

First Edition

Publication year: 2023

ISBN 978-80-7678-219-8

